DRAG OF FREE-FALLING SPHERES IN DILUTE AQUEOUS SOLUTIONS OF POLY (ETHYLENE OXIDE) FOR REYNOLD NUMBERS ABOVE THE CRITICAL VALUE

by

Edgar Franklin Woolery

UNITED STATES
NAVAL POSTGRADUATE SCHOOL

THESIS

DRAG OF FREE-FALLING SPHERES IN DILUTE AQUEOUS SOLUTIONS OF POLY(ETHYLENE OXIDE) FOR REYNOLDS NUMBERS ABOVE THE CRITICAL VALUE

by

Edgar Franklin Woolery

December 1968

DRAG OF FREE-FALLING SPHERES IN DILUTE AQUEOUS SOLUTIONS OF POLY(ETHYLENE OXIDE) for REYNOLDS NUMBERS ABOVE THE CRITICAL VALUE

by

Edgar Franklin Woolery
Commander, United States Navy
B.S., University of Missouri, 1961

Submitted in partial fulfillment of the
requirements for the degree of

MASTER OF SCIENCE IN PHYSICS

from the

NAVAL POSTGRADUATE SCHOOL
December 1968

ABSTRACT

Drag of free-falling spheres in water and in dilute aqueous solutions of poly(ethylene oxide) was measured by ejecting the spheres near terminal velocity in a fluid-filled tank. Polymer additive concentrations tested were 1000 wppm, 200 wppm, and 100 wppm. The results agree with previous investigations, available only for subcritical Reynolds numbers, in that the drag coefficient decreases with increasing water Reynolds number and decreasing polymer concentration. It is shown that in the polymer solutions abrupt decrease in drag coefficient occurs at about the same Reynolds number (3×10^5) as the critical value in water. For Reynolds numbers greater than the critical value, the drag was still less than in water and increased slightly with increasing polymer concentration. At Reynolds numbers between 7 and 8×10^5, the drag coefficients for all polymer concentrations, including water, abruptly increased to nearly a common value at the upper limit of this investigation.

TABLE OF CONTENTS

LIST OF TABLES

LIST OF ILLUSTRATIONS

LIST OF ABBREVIATIONS AND SYMBOLS

c	Concentration of solute in a solution
C_D	Drag Coefficient for Cylinders or Spheres
C_{DF}	Skin Friction Component of Drag Coefficient of Cylinders
C_f	Flat Plate friction coefficient
C_m	Moment Coefficient for Torque on Rotating Disk
d	Diameter of Sphere, Cylinder
D	Diameter of Pipe
db	Decibel
dp/dx	Pressure Drop Per Unit Length of Pipe
f	Fanning Friction Factor for Pipe Flow
g	Acceleration due to Gravity
HEC	Hydroxyethylcellulose
K	A Constant in the Power-Law Model for Fluids
K_1	Virtual Mass Coefficient for an Accelerating Sphere
L/D	Length-to-Diameter Ratio for Cylinders
M	Molecular Weight
n	A Constant in the Power-Law Model for Fluids, Index of Refraction
n'	Index of Refraction
PEO	Poly(ethylene oxide)
PIB	Polyisobutylene
PMMA	Polymethylmethacrylate
$\Delta P/L$	Pipe Flow Pressure Drop in Pipe Length L
r	Disk Radius
Re	Reynolds Number
Re'	Generalized Reynolds Number

R_L	Reynolds Number Based on Length of a Flat Plate
R_L'	Generalized Reynolds Number Based on Length of a Flat Plate
$S_{0.99}$	Distance for Attainment of 99% of Terminal Velocity by a Free-Falling Sphere
S(I)	Distance Between Light Planes of Optical Velocimeter
u	A Component of Fluid Velocity in Pipe Flow
U_∞	Fluid Velocity Far From a Flat Plate
v_*	Friction Velocity in Pipe Flow, $v_* = (\tau_o/\rho)^{1/2}$
wppm	Weight Parts of Solute per Million Parts of Solvent
X	Empirical Factor for Drag Coefficients of Spheres in Stokes Flow in Power-Law Fluids
y	Displacement Between Fluid Elements or Between an Element and a Bounding Surface
α	A Constant in the Ellis Model for Fluids, A Pipe Flow Parameter Dependent upon Concentration of Polymer Additive
γ	Strain
η	Shear Viscosity of Solution
η_o	Shear Viscosity of Solvent
$[\eta]$	Intrinsic Viscosity
κ	Prandtl's Mixing Length Constant
λ	Friction Coefficient for Pipe Flow
λ_1, λ_2	Experimentally Determined Relaxation Times in a Constitutive Equation for Viscoelastic Fluids
μ	Shear Viscosity
ν	Kinematic Viscosity
ρ	Density of Fluid
ρ_s	Density of Sphere
ρ_w	Density of Water
τ	Shear Stress

τ_o	Shear Stress at a Wall or Bounding Surface
ϕ_c	Critical Angle for Refraction
ω	Angular Velocity

ACKNOWLEDGEMENTS

The very patient guidance and encouragement by Dr. J. V. Sanders in this investigation is gratefully adknowledged. This was particularly important in the development of the "infernal machine", which later acquired the more sophisticated name, "optical velocimeter". The assistance of LCDR J. W. Kinnier, who performed the viscosity determinations associated with this investigation and spent many hours retrieving spheres from sticky POLYOX solutions, is very much appreciated. The very able technical support by Mr. W. Smith, Mr. M. Andrews, and Mr. M. O'Dea is acknowledged with deep gratitude.

1. Introduction

1.1 General. Drag reduction (or friction reduction) by use of polymer additives in a flowing liquid has only recently begun to be developed. In 1944, Vanoni (61) observed that in a flume suspended sediment tended to appreciably reduce the turbulent transfer of momentum and hence the resistance to flow. This effect, which seemed to depend upon sediment concentration, allowed the sediment laden water to flow more rapidly than a comparable clear water flow. Then, in 1948, Toms (51) reported correlation between concentration and increased flow-rates (at constant pressure gradient) for turbulent flow of a high molecular-weight polymer solution in a circular pipe. Since this was apparently the earliest positive correlation between friction reduction and the concentration of polymer additive, the effect was termed the "Toms' phenomenon" by various authors. After Tom's report, although considerable effort was given to the study of the rheological properties of non-Newtonian fluids, little interest was evidenced in literature concerning the friction reduction properties of these substances until the late 1950's when the possibilities of practical uses for the Tom's phenomena began to be realized. Petroleum companies became interested when it was demonstrated that by introducing minute quantities of certain high molecular-weight polymers into pipelines the power required and thus the cost to pump petroleum or other fluids could be considerably reduced (7, 58). Other chemical process industries became interested in friction-reducing additives for the same reason.

1.2 Waterborne Vehicles. Another obvious potential for friction reduction was in applications to waterborne vehicles and the works of many researchers are reported in shipbuilding journals and reports of agencies connected with naval engineering. In order to study friction reduction on water vehicles, the problem was sometimes regarded as friction of a flat plate plus drag due to the wake generated as the vehicle moved through the water. Granville (17), assuming that practical drag reducing substances were non-Newtonian, applied ideas that had been developed by Metzner and his associates (32) for non-Newtonian additives in pipe flow to flat plates. He predicted a decided drag reduction for flat plates in a flowing non-Newtonian power-law fluid. Vogel and Patterson (62) reported drag reduction resulting from injecting poly(ethylene oxide), (POLYOX), solutions into the boundary layer of a three-dimensional streamlined model. They correlated drag reduction with polymer concentration and observed that the drag reduction increased with increasing molecular weight of the linear polymer used. Kowalski (25) observed significant drag reduction on ship models and flat plates towed in a tank containing very dilute solutions of POLYOX. Although he referred to this fluid as being non-Newtonian conventional viscometry indicates that even at high rates of shear these dilute solutions of polyox are Newtonian. A further demonstration of drag reduction by "non-Newtonian" additives for water vehicles was given by Thurston and Jones (50,18) who tested a torpedo shaped vehicle having a soluble coating of high molecular-weight polymer on its nose section. Merrill, Smith, and Chung (31) reported drag reduction on both a flat plate and a torpedo shaped body for low concentrations of polyox in water. However, drag on the "torpedo" increased for high polymer

concentrations. This was explained by assuming that the boundary layer had been laminarized so that early separation occurred and thus a larger diameter wake led to increased pressure drag.

Although, in principle, drag reduction for water-borne craft can be accomplished, utilization of the principle on a full scale may not be practical unless the efficiency of the process is such as to allow practical quantities of polymer to be employed. Kowalski (25) estimated that to reduce drag on a typical 450 foot merchant ship at a speed of 18 knots would require injecting on the order of 13000 lb/hr. He pointed out the obvious fact that continuous application of this additive would not likely be at all practical. However, the use of additives for short bursts of speed in large vessels or continuously in much smaller vehicles might be more feasible. These examples of work in the field of drag reducing additives indicate that ample motivation is present for continuing study of these substances. By gaining more insight into the nature of turbulent friction reduction not only will more practical utilization of the principle be realized but it is likely that greater understanding of turbulence itself may result.

1.3 Fluid Dynamic Drag and Drag Reduction. The drag force or resistance to motion of a totally submerged body moving through a fluid is usually thought of as consisting of resistance due to skin friction plus profile drag due to a negative pressure developed in the wake behind the body. Skin friction and profile drag, taken together, are often referred to as viscous drag. In the case of bodies moving in water and which are not fully submerged an additional drag or resistance component known as wave drag affects the motion of the body. Wave drag results from surface

wave effects and surface spray effects. Since men began using ships and various water vehicles, attention has been given to methods of reducing the resistance to motion of the vehicles through water. Until recently the efforts have been largely confined to wave and profile drag by reducing frontal area or to reducing skin friction by smoothing surfaces exposed to the fluid and by controlling the fluid flow around the body so that the boundary layer remained laminar. As mentioned above, the possibility of using polymer additives to reduce the viscous drag has generated considerable interest in the investigation of fluids containing these additives.

The analysis of fluid flow past various simple geometrical shapes has often provided insight into solution of problems of flow past more complicated but more practical shapes. The resistance to flow past a flat plate or resistance to flow in pipes is almost entirely due to skin friction. There is no profile drag due to a wake nor is there a boundary layer separation. On the other hand, except for flows with very low Reynolds number, profile drag is predominant for flows past spheres and past cylinders oriented normal to the direction of flow. Thus, by a suitable choice of model shapes various contributions to the resistance to fluid flow can, to some degree, be "isolated".

Although this investigation is primarily concerned with drag reduction for spheres, a brief summary of those fluids flow characteristics affecting drag for flows in various geometries is presented in order that drag or friction reduction may be viewed in broad perspective. In particular, much emphasis is given to pipe flow, largely because of the abundance of work reported for friction reduction in pipe flow. This, in turn, is due to the relative ease in performing pipe flow measurements and the difficulty

of conducting experiments with other shapes. In addition, topics discussed in the summary will enhance understanding and interpretation of sphere drag reduction.

1.3.1. Rheology. The relationship, called the constitutive equation, between flow parameters and the shear stress exerted by the fluid upon a bounding surface or between adjacent fluid elements is an essential element in an analysis of viscous drag. For those fluids which are called Newtonian and can be considered incompressible this relationship for a one-dimensional flow is:

$$\tau = \mu(du/dy)$$

where τ is the shear stress, μ the constant shear viscosity of the fluid, u the component of velocity normal to y, the direction of displacement between the fluid element and the bounding surface or between the adjacent fluid elements. A plot of shear stress with rate of shear, τ versus du/dy, for Newtonian fluids is linear. Those fluids which do not have this linear flow curve are collectively called "non-Newtonian". Flow curves for some fluids which are encountered among various time-independent fluids are shown in Fig. 1.1. See Skelland (48). A Bingham plastic exhibits a constant fluid viscosity but only after a "break-out" shear is applied. The pseudoplastic flow curve characterizes most non-Newtonian fluids. These fluids are often called shear thinning, which seems appropriate upon noting the shape of the flow curve. A few fluids, sometimes termed "shear thickening", are characterized by the "dilatant" fluid flow curve type. Many fluids, over a restricted range of shear rates can often be characterized by the so-called power-law or Ostwald-de Waele model:

$$\tau = K\,(du/dy)^n$$

where n and K are experimentally determined constants. Obviously this model is valid only for those values of shear rates which produce linear log τ versus log du/dy plots. Newtonian fluids represent the special case of a power-law fluid with n = 1 and K the shear viscosity. Shear thinning fluids have $0 < n < 1$ and K can be thought of as an apparent viscosity although, since this is empirical, no physical significance can be inferred. Another important group of non-Newtonian fluids exhibit time dependence in that they have both viscous properties and elastic properties. When subjected to stress these fluids flow, but when the stress is removed they tend to partially recover. For these fluids the constitutive equation given by Skelland (48) and attributed to Fröhlich and Sack (11) and Oldroyd et. al. (35) is

$$\tau + \lambda_1(d\tau/dt) = \mu^*[(d\gamma/dt) + \lambda_2(d^2\gamma/dt^2)]$$

where λ_1 and λ_2 are experimentally determined relaxation times, γ is the strain, and μ^* is an experimentally determined viscosity which at very low rates of shear is the Newtonian viscosity. It is noted that for a purely viscous fluid, i.e., a fluid having no significant elastic properties, this equation reduces to that given above for the Newtonian case since $\lambda_1 = \lambda_2 = 0$ and for low strains $d\gamma/dt = du/dy$. For high rates of shear, a constitutive equation containing higher order terms and five additional experimentally determined constants has been derived by Oldroyd et.al. (35).

The drag reduction phenomenon produced in fluids containing even trace quantities of polymer additives are not readily explained by accepted descriptions of Newtonian flow. Thus, these fluids are

classified as non-Newtonian, although there is evidence (9) that, in terms of conventional viscometry, drag reduction occurs in some fluids which appear Newtonian.

1.3.2. Pipe flow. For flow in circular pipes a friction coefficient is defined as:

$$\lambda = (-dp/dx)\ D/(\tfrac{1}{2}\rho V^2)$$

where dp/dx is the drop in pressure per unit length of pipe, D the pipe diameter, ρ the fluid density, and V the mean fluid velocity in the pipe. If a Reynolds number is defined as $Re = VD/\nu$ where ν is the Newtonian kinematic viscosity of the fluid then it has been shown, both by solution of the Navier-Stokes equations and by experiment, that for laminar flow of a Newtonian fluid:

$$\lambda = 64/Re$$

This is often called Hagen-Poiseuille flow. This expression for pipe friction coefficient generally has been observed to be valid for Reynolds numbers less than about 2100 although the exact transistion Reynolds number depends upon the degree of success achieved in injecting the fluid into test sections without generating flow disturbances leading to turbulence.

For fully developed turbulent flow in pipes, no general and exact solution of the Navier-Stokes equations is available; however, semi-empirical expressions have been developed. Prandtl's mixing length hypothesis and his assumption of a simple form for the mixing length, $l = \kappa y$ led to a universal velocity distribution law for the flow of Newtonian fluid characterized by large Reynolds members:

$$(\bar{u}/v_*) = (1/\kappa)\ln(yv_*/\nu) - B$$

where $\bar{u}$ is the time average fluid velocity at a point, v_* the friction velocity = $(\tau_o/\rho)^{1/2}$, τ_o the tangential wall stress, y the distance from the pipe wall locating the point at which the velocity is $\bar{u}$, and κ and B constants of integration which must be determined experimentally. Prandtl's universal law of friction for smooth pipes can be obtained from the universal velocity distribution law given above.

$$1/\lambda^{1/2} = 2.0 \log(Re\ \lambda^{1/2}) - 0.8$$

The constants in this expression result from setting $\kappa = 0.4$ and $B = 5.5$ in the universal velocity distribution law. These values produce expressions which best agree with velocity profiles and friction coefficients observed for the flow of water in smooth pipes.

Dodge and Metzner (8) developed empirical friction-coefficient expressions for turbulent pipe flow for fluids whose constituitive equation could be approximated by the power-law model. This empirical expression was:

$$1/f^{1/2} = [4.0/(n')^{0.75}] \log (Re' f^{1-n'/2}) - 0.40/(n')^{1.2}$$

where n' is the flow behavior index, f is the Fanning friction factor ($f = \lambda/4$), and $Re' = (D^{n'} V^{2-n'} \rho)/(g\ K' 8^{n'-1})$ is a generalized Reynolds number. The flow behavior index is determined experimentally from:

$$n' = d(\log(D\Delta P/4L))/d(\log(8V/D)).$$

The constants are further related by:

$$\tau_o = D\Delta P/4L = K'(8V/D)^{n'}$$

where $\Delta P/L$ is pressure drop in a length, L, in the pipe. For pipe flow these constants can be related to the power-law constants by:

$$n' = n$$

$$K' = ((3n + 1)/4n)^n$$

Metzner and his associates (32) had previously shown that for laminar pipe flow, $f = 16/Re'$ or $\lambda = 64/Re'$. Although the power-law model has often been useful, many fluids of interest as drag reducers are not well described by this general expression (8,45). In addition, those fluids having significant elastic properties would not be expected to behave according to this description.

As has been mentioned previously, many fluids in which drag reduction occurs are essentially Newtonian. Some researchers have attempted to determine new constants for the Prandtl friction law for various concentrations of additives in fluids (16) or have correlated friction coefficients using, as parameters, $1/f^{1/2}$ and $Re(f^{1/2})$. Incidental to determining empirical constants for the friction law of POLYOX WSR 301, Goren and Norbury (16) determined mixing length values for various additive concentrations and distances from the pipe wall. Many workers have suggested the likelihood (16,21, 39) that the drag reduction observed for turbulent pipe flow results from viscoelastic effects, although the elastic effects are difficult or impossible to observe by the usual methods.

One of the problems associated with these investigations was that some polymer additives degraded in turbulent flow thereby altering the drag reduction properties. Some of the fluids were clearly viscoelastic when containing polymer additives in excess of about 0.1% (1,000 weight parts per million, wppm) but the concentrations employed in many of the investigations were on the order of only a few wppm. Because of these

problems and because of the apparent Newtonian character of many of the drag reducing fluids, the explanation of drag reduction by viscoelasticity has not been universally accepted.

In an analysis of the effect of polymer additives on turbulent wall friction F. M. White (66) attributed to Meyer the observation that the constant, B, in the universal velocity distribution law for pipe flow, changes upon addition of polymer if the friction velocity exceeds some threshold value, v_o^*. Meyer gave an approximation for B as: $B \doteq 5.5 + \alpha \ln(v^*/v_o^*)$ where α is a dimensionless constant dependent upon the type of additive and the concentration. The constant κ is apparently unaffected by polymer additives. White gives α for POLYOX WSR 301 solutions:

$$\alpha = 3c^{0.57}$$

where c is polymer concentration in wppm. Some of the typical friction coefficients observed for various fluid types flowing in pipes assumed to be smooth are given in Figs. 1.2, 1.3, and 1.4. The solid lines denote curves for pure solvent and the dotted lines represent behavior of the fluid with additives. In each case, it is significant that in the laminar flow region the additive does not change the fluid friction. Hershey and Zakin (21) noted that a fluid containing drag reducing additives remained in laminar flow until a greater Reynolds number had been achieved than for the pure solvent. For fully turbulent pipe flow a second kind of drag reduction takes place. In figures 1.3 and 1.4, A, B, and C represent different concentrations. The primed letters of figure 1.3 denote flow in smaller diameter pipe than that for the unprimed letters. The "critical" Reynolds number for drag reduction in turbulent flow has been shown to be dependent upon pipe diameter (9,21,39) and independent of polymer concentration (16). Ram attributed this to a relaxation within the polymer chain.

1.3.3. Flow past flat plates. In the case of the two-dimensional boundary layer flow along a flat plate at zero incidence the friction coefficient is defined as:

$$C_f = \tau_o / (1/2\ \rho U_\infty^2)$$

where U_∞ is the fluid velocity far from the plate. The velocity profile for smooth flat plates can be written in a logarithmic form similar to that given for turbulent pipe flow but it is usually more convenient to express flat plate resistance coefficients empirically such as the Prandtl-Schlicting skin friction formula:

$$C_f = 0.455/(\log R_L)^{2.58} - A/R_L$$

where R_L is Reynolds number based on the length, L, of the plate; $R_L = U_\infty L/\nu$. For laminar boundary layer flow along a flat plate, the Blasius formula, $C_f = 1.328/R_L^{1/2}$ applies. Granville (17) developed friction coefficients for flat plates in power-law fluids. For laminar flow:

$$C_f = 2(0.824)^{1/(n+1)}[(n+1)^{2+1/n}/(2n+1)(3n+2)]^{n/(n+1)}/R_L'^{n/(n+1)}$$

where n is numerically equal to the value determined in pipe flow experiments R_L' is the generalized Reynolds number based on length of the plate,

$$R_L' = (U^{2/n-1}L)/(K/\rho)^{1/n}$$

For turbulent flow:

$$C_f = P^2/(\log R_L'^n - Q)^2$$

where P and Q are empirically obtained. Van Wijngaarden (60) as well as Acrivos et. al. (1) following Granville, presented an analysis of laminar boundary layers for power-law fluids. F. M. White (66) used

data from pipe flow to predict friction coefficients for turbulent flow along flat plates. He observed that, as shown in Fig. 1.5, reduction in local skin-fraction coefficient would be expected in laminar flow as well as in turbulent flow, however, contrary to observation in pipe flow, the turbulent friction reduction would decrease with increasing solvent Reynolds number and with decreasing α, a parameter determined from pipe flow data. At some point no drag reduction would occur for further Reynolds number increase.

1.3.4. Torque on Rotating Disks. A circular disc rotating about its axis normal to the surface is a convenient device for investigating drag reduction. The torque on the disc is entirely due to skin friction and this torque can be easily measured. For a rotating disc in a stationary fluid, a moment coefficient is defined as:

$$C_m = (\text{torque on both wetted sides of disk})/(1/2\rho\omega^2 r^5)$$

with ω the angular velocity and r the disk radius. Schlicting (43) gives for Newtonian laminar flow:

$$C_m = 3.87/Re^{1/2}$$

where the Reynolds number, $Re = r^2\omega/\nu$. For turbulent flow Goldstein (15) developed a moment coefficient for rotating disks of the same form as the universal resistance law for pipes:

$$1/C_m^{1/2} = 1.97 \log (Re\, C_m^{1/2}) + 0.03.$$

Hoyt and Fabula (23) found that, within the scope of their investigation, increasing the concentration of poly(ethylene oxide) up to 621 wppm produced increasing drag reduction. The trend, as shown in Fig. 1.6 seems to be that turbulence is suppressed, moving the flow conditions toward laminar Newtonian flow.

1.3.5. Flow Past Bluff Bodies. Drag exerted by a fluid flowing past a bluff body is more difficult to analyze than friction in pipes or on flat plates. Therefore, analytical expressions for cylinder and sphere drag coefficients such as those by Lamb, Stokes, and Oseen have been developed only for very low Reynolds numbers. Numerical solutions such as that for spheres given by Jensen (24) are available for Reynolds numbers up to about 40. Beyond this, general analysis is not very practical. In pipe flow and flow past flat plates only skin friction was involved in the resistance to fluid motion. On the other, flows past bluff bodies at high Reynolds numbers are characterized by vortex formation and shedding accompanied by boundary layer separation. This leads to formation of a wake and a negative pressure which acts as a retarding force, termed form or pressure drag. In addition, as Reynolds number is increased the boundary layer changes from laminar to turbulent. Both cylinders and spheres exhibit sudden decreases in drag coefficient at a Reynolds number referred to as the critical Reynolds number. Drag coefficients are defined as:

$$C_D = (\text{drag force/unit length})/(1/2\rho U^2 d) \quad \text{for cylinders,}$$

$$C_D = (\text{drag force})/(1/2\rho U^2)(\pi d^2/4) \quad \text{for spheres,}$$

and Reynolds numbers are $Re = Ud/\nu$ (for both cylinders and spheres), where d is diameter and U is free stream fluid velocity. In both cases the critical Reynolds number occurs around 3×10^5 the exact value depending upon surface roughness and turbulence in the fluid. The curves shown in Figs. 1.7 and 1.8 are drawn to indicate most commonly encountered critical Reynolds numbers and largely represent the work of Weiselsberger as presented in current literature such as that of Schlicting (43) and Hoerner (22).

For very low Reynolds numbers, skin friction is a significant component of drag for bluff bodies. For spheres, Stokes' solution shows that two-thirds of the drag at low Reynolds numbers is due to skin friction. Goldstein (15) gives an expression for cylinder skin friction as $C_{DF} = 4/Re^{1/2}$ which is valid for $30 < Re < 10^4$ and at Re = 10 Goldstein says Thom determined that skin friction accounts for about 43% of the drag. As Reynolds numbers are increased and wake size increases, pressure drag becomes the significant contributor to drag of bluff bodies. Upon further increase of Reynolds number, the boundary layer becomes turbulent, the point of separation of the laminar boundary layer from the body surface is shifted abruptly toward the rear, and drag is reduced by the resulting reduction in wake size. In the case of cylinders, Roshko suggested that this shift rearward is actually a reattachment of the boundary layer to the surface forming a bubble which he called a separation bubble followed by a second separation further toward the rear. Sanders (42) suggests the possibility of the same mechanism working for spheres also.

Because of the ability to assume a two-dimensional boundary layer, cylinders, at first, appear simpler for investigation than spheres, but complications arise because of end effects and the periodic shedding of vortices which give rise to oscillatory forces transverse to the direction of flowing fluid. Consequently, an infinite length-to-diameter ratio (L/D) must be assumed to obtain a generalized plot of cylinder drag coefficients with Reynolds number. If one works with cylinders whose L/D is small he must either apply some correction factor or state the value of L/D for which his results are valid.

The degree of difficulty in handling Newtonian flows about bluff bodies suggests that to further complicate the problem by disallowing the Newtonian assumption for a constituitive equation would bring about insurmountable analysis difficulties and, to date, this has been the case. Investigations of non-Newtonian flow about cylinders are represented by a few applications of two-dimensional boundary layer solutions such as that by Acrivos, et al (1) for power-law fluids and a few experimental investigations of fluids containing drag reducing additives such as that by McClanahan and Ridgely (27). The latter authors reported drag enhancement for Re less than about 10^4 and drag reduction for greater Reynolds numbers. Although the scope of their work did not extend to the critical Re, the trend of their results as sketched in Fig. 1.9 suggested that, in fluids containing drag reducing additives, there might be no "drag crisis", as the sudden drop in drag coefficient at the critical Reynolds number is sometimes called.

Spheres in non-Newtonian fluids have enjoyed slightly more attention than have cylinders. For very low Reynolds numbers, Skelland (48) gives for power-law fluids:

$$C_D = 24\ X/(d^n U^{2-n} \rho/K)$$

where X is a function of n and is determined experimentally. This expression is not very satisfying in that many variations in X have been found by various investigators. Slattery and Bird (49) presented another analysis for sphere drag coefficients at very low Reynolds number for fluids which are characterized by the Ellis Model:

$$\tau = (du/dy)/(A + B\tau^{\alpha - 1})$$

where A, B, and α are constants to be evaluated empirically. Bizzell and Slattery (4) calculated boundary layer separation points on spheres as a function of n, the power-law model exponent. Turian (57) applied the Ellis model to one to two percent aqueous solutions of poly(ethylene oxide), and hydroxyethyl cellulose, in an investigation of spheres in creeping flow. These theoretical results provide some insight into behavior of non-Newtonian fluids but they do not allow prediction of the behavior of fluids containing drag reducing additives for flows characterized by fully developed wakes and separated boundary layers.

Drag reduction has been reported by various researchers as well as drag enhancement in a few cases for spheres in fluids with polymer additives. These results have been summarized by Sanders (42) and the general trend is shown in Fig. 1.10. A.White (64) performed a particularly interesting experiment by roughening the surface of a sphere so as to artifically "trip" the boundary layer into turbulence and thereby produce minimum pressure drag in water. Dropping the sphere in a very dilute aqueous solution of poly(ethylene oxide) he observed a drag increase. His explanation was that the polymer additive had suppressed the boundary layer turbulence and caused the pressure drag to return toward the value of drag obtained prior to roughening the sphere surface.

1.4 Drag Reducing Polymers

1.4.1. General. In the foregoing summary of fluid drag it was apparent that most investigators had failed to correlate drag reduction with non-Newtonian behavior. In some cases polymer solutes were sufficiently concentrated that the power-law model or Ellis model

could be applied with slight success but, in general, drag reduction had to be attributed to something other than just a variation in rheological properties. It has been suggested by Hoyt and Fabula (23), Hershey (21), and others, that a possible explanation might be that viscoelastic effects in even apparently Newtonian fluids are responsible for turbulence suppression and consequent reduction of skin friction of pipe flow, flow past flat plates, and rotating disks. In the case of bluff bodies the viscoelastic effects would be assumed to reduce turbulence in the wake and delay separation of the laminar boundary layer causing reduced pressure drag.

A wide variety of polymers have been used as drag reducers. Among the most commonly used in water are poly(ethylene oxide) (PEO), guar gum, polyacrylamide (SEPARAN), carboxymethyl cellulose (CMC), and hydroxyethyl cellulose (HEC). Polymers used in other fluids are poly(methylmethacrylate) (PMMA) in toluene and in monochlorobenzene and polyisobutylene (PIB) in kerosene and in cyclohexane. Hoyt and Fabula (23) reported results of drag reduction tests on twenty-eight different polymer additives and five natural substances. Those producing the most dramatic drag reduction were PEO (WSR-205), guar gum, and SEPARAN. For 70% torque reductions on a rotating disc at $Re = 1.3 \times 10^5$, concentrations in wppm required were 250 for WSR-205, 500 for guar gum, and 100 for SEPARAN AP-30. In other tests of the same investigation they observed that other forms of PEO having higher molecular weights, WSR-301 and COAGULANT, gave even more striking results. In concentrations in excess of about 0.1% many drag reducing additive polymers cause the resulting fluids to exhibit measurable viscoelasticity, and a significant portion of the work done with drag reducers has been at these concentrations. Of special note, however, is that PEO and guar

gum, as well as several of the others, yield greater drag reduction when present in concentrations on the order of 100 wppm, and less, than when concentrations are such that viscoelasticity can be measured. For all geometries it has usually been reported that drag reduction increased with concentration to some maximum drag reduction, and then decreased with further increase in concentration.

It has been generally observed that drag reducers have very long-chain molecular structures and have very large molecular weights, on the order of 10^6. Quite appropriately they are often referred to as macromolecules. High molecular-weight polymers having chain structures with many appendages or highly coiled chains, generally have not produced as dramatic drag reductions as have those whose structures are simple (38). The solubility of the additive also affected the drag reduction (23). It must be recognized that temperature and presence of inorganic salts often dramatically affect chain coiling which in turn affects polymer solubility. Another, sometimes annoying, property of some high molecular-weight polymers is their susceptibility to degradation. It has been found that many polymers are reduced in size by chain scission brought about by oxidation, turbulence, droplet formation, and sound waves. This degradation, if it occurs in the course of a drag reduction experiment, often makes interpretation of the results difficult, especially if one is attempting to correlate molecular weight with drag reduction. Determination of the degree of degradation during an experiment is not as easy task. One must first solve the problem of taking a representative sample and then determine molecular weight by some means such as by determining intrinsic viscosity. The degraded polymer's molecular weight

is then calculated from the widely accepted empirical relationship:

$$[\eta] = kM^{0.78}$$

where $[\eta]$ is the intrinsic viscosity, k is a temperature dependent parameter, and M is the molecular weight. The intrinsic viscosity is defined as:

$$[\eta] = \lim_{c \to 0} ((\eta - \eta_o)/\eta_o c)$$

where $\eta = \mu$, the shear viscosity of the solution, η_o is the solvent viscosity, and c is the solute concentration expressed in grams per 100 ml.

1.4.2. Poly(ethylene oxide). Poly(ethylene oxide), also called polyoxyethylene and polyoxirane, is an addition polymer of ethylene oxide and has molecular weights ranging between 100,000 and 10 million. Lower molecular weight ethylene oxide polymers are usually known as polyethylene glycols. Union Carbide Chemicals Company presently is the sole manufacturer of PEO and the polymer is marketed as "POLYOX" in several molecular weight ranges, some of which are listed in Table I. Powell and Bailey (36) note that PEO has several properties which vary from those expected of glycols and these apparently result from the extremely long molecular structure. The resin is water soluble at room temperature but has an inverse temperature solubility relationship; i.e., as temperature increases, solubility decreases. Presence of various salts such as sodium phosphate and sodium carbonate can significantly lower the solubility of PEO in water. It is soluble in aromatic solvents but insoluble in aliphatic hydrocarbons and glycerin. Aqueous solutions of PEO at concentrations of 1% and greater are pseudoplastic and definitely are not thixotropic. Solutions with concentrations on the order of

100 wppm are Newtonian for shear rates less than about 10^6 sec^{-1} (23). McGary (29) found that POLYOX degrades upon standing in solution as well as under influence of turbulence and ultraviolet light. Degradation in solution also occurs in the presence of various oxidizing agents such as potassium permanganate and hydrogen peroxide. The mechanism of this latter degradation is thought to be autoxidation initiated by ferrous, cupric, cuprous, and silver ions in addition to the agents mentioned above. The quality of tap water affects the stability of PEO solutions. Water containing chlorine and metallic salts in general yields solutions having poorer stability, than distilled water solutions. McGary also confirmed that certain alcohols stabilized PEO and reduced degradation. Pruit, Rosen, and Crawford (38) observed degradation of WSR-701 Resin when stored for long periods of time.

2. Determination of Drag Coefficients of Spheres

2.1 Motivation for Experiments with Spheres. Although much has been done in studying drag reduction in pipe flow, comparatively little has been reported regarding drag reduction on bluff bodies. While the phenomenon is not very well defined for any geometry, the need for much more experimentation with bluff bodies in separated boundary layer flow of drag reducing fluids is most apparent.

Pipe flow experiments and rotating disc experiments usually can be carried out without great difficulty; however, experiments with bluff bodies present special problems that must be solved if meaningful results having general interpretations are to accrue. As was mentioned earlier, drag of totally submerged cylinders can be greatly affected by L/D. Other complicating problems associated with cylinders encountered by McClanahan and Ridgely (27) were ventilation behind the strut supporting the test cylinder as well as the contribution to drag by the strut itself.

The fluid containers in which bluff body tests are conducted frequently affect the results in some way. For creeping flow, very low Reynolds numbers, the presence of bounding surfaces within several diameters from the test body can cause a significantly higher value of drag coefficient to result (19,28). For tests with separated laminar boundary layers on bluff bodies, the walls of a tunnel cause turbulence in the fluid which may alter the character of the laminar boundary layer. This effect has been particularly noticeable (15,22,43) for Reynolds numbers in the vicinity of the

drag "crisis". According to Torobin and Gauvin (53) it was not until the completion of the wind tunnel at Goetingen that Weiselsberger, in 1922, was able to conduct tests on spheres without being affected by turbulence originating at the tunnel walls.

Attempts to surmount this difficulty were made by observing spheres during free fall. While in tunnel tests, the body is supported rigidly by a strut and drag force measured directly, in the free falltests terminal speed is determined and the drag force calculated. At terminal speed the accelerating force of gravity on a sphere is balanced by the retarding force exerted by the fluid plus the buoyant force of the fluid:

$$(4/3)\pi(d/2)^3 \ (\rho_s - \rho_w)g = \text{drag}$$

where ρ_s is the density of the sphere, ρ_w the fluid density, U the terminal velocity and g the acceleration due to gravity. The drag coefficient is then:

$$C_D = (4/3)g\ d(\frac{\rho_s}{\rho_w} - 1)/U^2 = A/Re^2$$

where A is a constant dependent upon sphere parameters and fluid density only. It is assumed that no unbalanced horizontal force acts on the sphere. If the sphere is accelerated,indicated by failure to reach terminal velocity or deviation from a vertical fall, then the above expression is invalid. Odar and Hamilton (34) presented an analysis for drag on an accelerating sphere in harmonic motion for Reynolds numbers below about 60 and later Odar(33)confirmed the applicability of the development to freely falling spheres.

According to Goldstein (15), Lunnon found that for free falling spheres at Reynolds numbers greater than about 3×10^4 and less than about 10^5 drag coefficients were greater than those obtained by wind tunnel tests. Bacon and Reid (2) observed for Reynolds numbers between about 3×10^5 and 4×10^6 only a gentle decrease in drag coefficient to a minimum value of 0.16 at a Reynolds number of 10^6 instead of the abrupt decrease to a minimum of about 0.08 at a Reynolds number 4×10^5 observed by others in wind tunnel tests. Lang and Patrick (26) reported results of free-fall tests in water consistent with Lunnon's for Reynolds numbers up to 2×10^5. Between 2 and 3×10^5 they reported an abrupt decrease in drag coefficient like that obtained by wind tunnel testing. For a Reynolds number of 2.5×10^5, the upper limit of their tests, they reported a drag coefficient of 0.15 with an apparent decreasing trend. In their tests some of the spheres used by Lang and Patrick did not attain terminal velocity. They, as did Hayes (20) and Chenard (5) later, corrected their data for acceleration by applying a virtual mass coefficient.

In the present study of drag reducing additives, spheres were chosen as the test shapes and drag determination by free fall in a stagnant fluid was chosen as the technique. The choice was based on need for sphere experimentation especially in the vicinity of drag crisis as well as the convenience of having available a 3-foot diameter steel cylindrical tank having a height of 6 feet. Poly(ethylene oxide)WSR 301 in water was selected as the test fluid since, for the range of Reynolds numbers of interest, more results are available for comparison. It is apparent that a sphere should

attain terminal velocity and a means for determining the value of that velocity as well as confirming that acceleration was indeed zero should be provided.

2.2. Methods for Determining Sphere Drag Coefficients. Previous investigators using free falling spheres have used various methods for velocity determination. Torobin and Gauvin (53) attribute to Allen, in 1900, a stereoscopic photography technique for measuring velocities of spheres in fluids. Shakespear, in 1914, made use of an electrical timing system for measuring velocities of small weighted celluloid spheres in an air tower, and Bacon and Reid (2) in 1924 determined velocities of spheres falling from aircraft by using a pair of recording theodolites. More recently, incidental to drag-reduction studies, Lang and Patrick (26) and Hayes (20) used multiple-image strobe-flash photography for velocity determinations of small spheres falling at Reynolds numbers below drag crisis in transparent tanks. A. White (64) used high-speed cine photography for larger spheres in a transparent tank. In an investigation reported by Ruszczycky (41), Kinnier used a series of coils surrounding a cylinder containing the test fluid to sense the change in magnetic field as the test shape passed each set of coils. Chenard (5) attached to a sphere a very small tether which turned a potentiometer producing an output voltage proportional to vertical displacement of the sphere. At terminal velocity, the voltage recorded on an oscillograph yielded a straight line plot and the slope of the line corresponded to the terminal velocity of the sphere. Thurston and Jones (50,18) tested a torpedo shaped body in a 20-foot high tank having nine stations located 2 feet apart, vertically. Each station had a sensor system allowing

detection of passage of the body. The sensor system was composed of a horizontal transparent slit with a light source shining through the slit into the tank and a pair of light sensitive resistors mounted level with the slit. These received light reflected back from a polished band on the torpedo as it passed the station. This system allowed a distance - time relation to be obtained and subsequent analysis to obtain velocity.

A technique employed by Goldstein and Kreid (14) was not directly applicable to this study but nevertheless stimulated interest in the possibility of altering the technique to fit the present task. They measured fluid velocity in a duct by measuring the doppler shift in laser light scattered from particles moving with the fluid. For this study, use of lasers for velocity determination was considered by doppler shift measurement, as well as by employment of a laser radar. Both ideas were abandoned because, in addition to technological complexity, the expected speeds of the spheres (1 to 9 meters per second) would not likely be determinable within the desired accuracy. Other techniques considered but quickly abandoned, were acoustic echo-ranging and doppler-shift measurement of a reflected acoustic pulse. The use of a photographic technique was considered and abandoned since the drop tank was opaque and some phenomenal trickery would have been necessary to photograph a reasonable field of view from inside the tank. In addition, it was desired that a data reduction scheme less cumbersome than photograph measurements could be achieved. It was decided that a technique similar to that employed by Thurston and Jones could be developed and would likely be the most practical of the velocity determination schemes considered.

The spheres listed in Table 2.1 were selected in order to yield data at Reynolds numbers greater than and less than that at drag crisis as well as to provide data within the range of boundary layer transition as shown in Fig. 2.1.

An additional problem which had not been solved was the question of how to cause a sphere to achieve terminal speed in the available drop tank. Estimates for the fall distances ($S_{0.99}$) required for spheres used in this study to attain 0.99 terminal speed shown in Table 2.1 were calculated using the expression developed by Lang and Patrick (26).

$$S_{0.99} = 2.62\ d/C_D\ (\rho_s/\rho_w + K_1)$$

In this expression K_1 is a theoretical virtual mass coefficient given as 0.5 for bodies not generating significant wakes and 1.8 when a wake was present. The estimates of Table 2.1 assumed $K_1 = 1.8$.

2.3 Optical Velocimeter. An optical velocimeter was built as an integral unit as shown in Figs. 2.1 and 2.2. Uniformly spaced planes of light radiated from two vertical lamp tubes flanking a single tube containing a light "receiver". A sphere falling through the planes of light reflect light to the receiver through collimating slits in an outer shell which surrounded the lamp tubes and the light receiver. The light receiver was an acryllic plastic rod contained concentrically inside an acryllic plastic tube. Light flashes received in the rod were transmitted along the rod to a multiplier phototube mounted at the top of the velocimeter. The series of output pulses from the phototube as the sphere passed through successive light planes could be recorded on magnetic tape or on an oscillograph producing a distance - time relationship for the falling sphere. By dividing the distance between two light planes by the time measured between pulses a rough mean velocity for that interval was obtained. If terminal

velocity was attained, this mean velocity is the value for the vertical component of the spheres velocity.

Prior to building the velocimeter described above, a small developmental model having only three slits was constructed and tested in order to assure feasibility of the velocity determination technique, and to develop optimum design parameters. The light receiver rod was notched at each slit as shown in Fig. 2.4 so as to provide for optimum light reception and to allow the acryllic rod to act as a light pipe to transmit the maximum amount of light to the phototube. It was experimentally determined that variation in the angle of the face of the notch produced variation in the photo-tube output. A "V" cut having an included angle of about 40° - 60° and a depth of cut approximately 1/6 of the rod diameter gave slightly greater output than other notches. Polishing the notch slightly diminished the output. Turning the rod so as to position the slit to the side opposite the incoming reflected light produced approxi-mately 30% increase in voltage output of the phototube. It was also determined that without the notch, no significant light reflection was received at the phototube. Misalignment of the notches behind the collimating slits by as little as 0.5 mm caused drastic reduction in the phototube output-pulse amplitude. This caused serious concern because the signal-to-noise ratio was low (about 15 db) even under optimum velocimeter operating conditions.

Light pipes are optical waveguides in that because of multiple internal reflection light trapped inside is transmitted along the "pipe" even though slight bends may occur. Two transparent media having a smooth interface and having different indices of refraction

will allow internal reflection. If a light ray incident on the interface in the medium having the higher refractive index, n', has an angle of incidence greater than the critical angle, ϕ_c, given by:

$$\phi_c = \sin^{-1} n/n'$$

where n is the refractive index of the second medium, then the ray will, in principle, be totally reflected. In practice, imperfections in the interface due to defects or contamination by dust and grease cause some light to be transmitted or leaked through the interface. For a short light pipe or even a long pipe transmitting very intense light this might not be a problem. Since the light reflections in the velocimeter would be of low intensity it seemed necessary to optimize the light receiver surface. The possibility of silvering the rod that would, in the final design, likely be approximately 6 feet in length, was considered. It was hoped that this would prevent contamination of the plastic surface and "help" the reflectivity somewhat. A commercial firm was consulted and because of the nature of the silvering process the acryllic plastic rod could be silvered only by very special treatment which, it was estimated, would cost on the order of $9000. Because of the cost involved and because it had been reported by Siegmund (47) that silvering could actually result in greater light leakage, the idea of a metallic coating was abandoned. Siegmund also reported that the best coatings for light pipes were dielectric substances having refractive indices less than that of the pipe but because of the expected small advantage no coating was specified for the velocimeter light receiver. For the velocimeter a low value of ϕ_c was desired for maximum light reception

or "trapping" and transmission. Since $\phi_c = \sin^{-1} n/n'$ the ratio of n/n' had to be minimized. Since the refractive index of the plastic was 1.5, that for water was 1.33, and that for air was 1.0, it was decided to encase the light receiver inside a water-tight acryllic-plastic tube which would allow the light pipe to function with a plastic-air interface and would give more favorable internal reflection than would a plastic-water interface. The rod would have considerably more than a few wavelengths separating it from the tube and thus no significant light leakage was expected.

The light source for the developmental velocimeter model was a pair of fluorescent tubes, one in each lamp cylinder. Immediately upon attempting to operate the device it was apparent that the electro-magnetic noise generated and radiated by the fluorescent process was excessive and completely obliterated any reflection pulse that might have been present in the phototube output. It was determined that a d.c. lamp would allow satisfactory operation if an adequately high intensity lamp could be found. The highest intensity d.c. lamps available with globe size of one-inch diameter or less was a 12-volt automobile instrument lamp, number 1073, which had a rating of 32 candlepower. The one-inch globe diameter was dictated because the lamp cylinders had been designed for a one-inch diameter fluorescent tube and, in addition, small lamp-cylinder size was desirable for good collimation with reasonably small overall diameter. Associated with the choice of light source was the problem of noise in the photo-tube output even with a d.c. light source. In order to obtain satisfactory velocimeter operation it was determined that the use of a low-pass filter connected to the phototube's cathode follower output was necessary. No satisfactory explanation of this is available

but apparently the very low light intensities reflected into the light receiver were inadequate to overcome dark current noise and other electronic noise in multiplier-phototube operation and the velocimeter pulses were distinguishable only by filtering. It was observed that if a sufficiently intense light source were beamed into the slits, "normal" phototube operation (without filtering) was possible, confirming, to some degree, the conjecture given above. Tests were conducted in which lamp intensity was varied by varying supply voltage, high voltage supply to the phototube was varied, and filter cutoff frequency was varied. For the model velocimeter, it was determined that the combination of parameters giving best results was: rated voltage on each of the lamps (12 volts), 1550 volts high voltage supply and, low pass 35 Hz and below in the filter. In other tests it was noted that the phototube output-pulse amplitude decreased very rapidly with separation between velocimeter and sphere. This decrease was found to be approximately proportional to the square of the sum of the distance between the light source and the sphere and between the sphere and the light receiver.

A Dumont 6291 multiplier phototube was used in the model development tests but it was determined that, although a Dumont 6292 had nearly the same characteristics, slightly improved velocimeter performance resulted by using the 6292 phototube. This latter tube is a 10 - stage multiplier phototube with a flat end - window type photocathode having its maximum response at about 4400 Angstroms. The response of this multiplier phototube was such that incandescent lamps with tungsten filaments provided a very good match with the chosen

multiplier phototube. De Vos (6) reported that the emissivity of a tungsten ribbon decreased very slightly in the wavelength range between 0.35 μ and 0.55 μ, which is the range of greatest sensitivity of the Dumont 6292 phototube. In this range, according to Planck's radiation formula, radiated energy increases with increasing wavelength and thus the lamps' spectral emission matched the spectral response of the phototube reasonably well. The Dumont 6292 multiplier phototube has an adjustable focusing shield allowing for optimum collection of photoelectrons. It has a minimum window diameter of 1.5 inches and a window index of refraction of 1.5 which is the same as that of the acryllic plastic rod from which light is transmitted to the phototube.

During testing of the model velocimeter the duration of the pulses produced as a sphere passed a light plane was approximately 10 to 12 msec. This is a much longer pulse duration than expected from slit geometry considerations and was probably caused by the use of the narrow-band filter at the photomultiplier output which led to longer circuit rise and decay times than would have resulted had no filter been used. Since it was desirable that each pulse be distinguishable, the required separation of light planes for a sphere falling at 8.6 m/sec was approximately 0.1 meter. Twelve light planes uniformly spaced at 0.108 m were specified for the final velocimeter as a compromise of the following:

1) Provide accuracy for measurement of time between pulses by large separation of the light planes.
2) Provide a maximum number of pulses to allow more samples for distance-time recording, and thus better resolution of velocity changes.

3) The velocimeter should not extend to the bottom of the tank since a sphere rebounding from tank bottom could cause extraneous signals which could interfere with analysis of valid pulses.

4) Light receiver rod should be of minimum length to avoid excessive light leakage and attenuation.

The optical velocimeter as shown in Figs. 2.1 and 2.2 had twelve 12 volt d.c. lamps in each lamp tube in 3 groups wired in series, each group consisting of four lamps in parallel. This allowed each lamp tube to be operated with its own power supply at 36 volts and 6.8 amperes. The lamps in each tube were mounted on a plastic strip as shown in Fig. 2.5 so that each lamp socket could be moved in its mounting block. This provided capability of positioning each lamp filament for uniform spacing or whatever filament spacing was required. In addition the plastic strip could be adjusted vertically for optimum position of the entire lamp assembly. Provision was made for a flow of cooling air within the lamp tubes to allow extended operation of the lamps if necessary with minimum danger of damaging the acryllic plastic tube and the insulation on the electrical leads to the lamps.

Optimum operation of the velocimeter was obtained by setting lamp tube voltage at 36 volts, multiplier phototube high voltage at 1050 volts, and the SKL Model 302 variable electronic filter set to pass frequencies of 120 Hz and below. The velocimeter outer casing was coated inside and outside with a light absorbing and diffusing velvet black paint. The aluminum lamp cylinders containing the lamp tubes as well as the aluminum cylinder containing the light-receiver assembly

was given the same finish. This was to prevent extraneous light reflections from interfering with proper velocimeter operation. The multiplier phototube was mounted inside an aluminum cylinder which also contained the cathode follower circuit for proper matching of the output with other electronic equipment used in conjunction with the system. A light-tight stainless-steel flange was designed to attach to the light-receiver cylinder and thread into the photomultiplier's aluminum cylindrical housing.

2.4 Sphere Ejector. In order that the test spheres achieve terminal velocity within the 6-foot drop tank, it was necessary to provide the spheres with an initial velocity. The optical velocimeter was to be positioned with its first light plane 6 to 8 inches beneath the fluid surface and it was desirable but perhaps not realizable to have the sphere at its terminal velocity as it passed the first light plane. An air-driven sphere-ejector system shown in Figs. 2.2 and 2.6 was built which catapulted a sphere downward, accelerating it from zero velocity just beneath the surface to near terminal velocity as the driving piston completed its downward travel. The ejector consisted of a cylinder and piston, sphere holder, accumulator, pressure regulator, and quick-action solenoid-operated valve. To the shaft of the piston was attached a short nylon rod which contacted the sphere. Sphere holders or "claws" of three sizes to accommodate the varying size spheres were constructed. Each had an aluminum base and three shaped phosphor bronze spring clips which held the sphere in position until the ejector shaft pushed the sphere from the holder. The sphere was ejected from a point 5 to 10 cm beneath the fluid surface so that "bubble capture" would be no problem.

2.5 Data Recording and Processing. Calculation of accurate drag coefficients and Reynolds numbers required maximum accuracy in measuring the time between recorded pulses and required that the distance between light planes be known accurately. The time between pulses was determined by recording the velocimeter output during the fall of the sphere at 37.5 inches-per-second (ips) on a Precision Instruments Model PI-6200 Instrumentation Tape Recorder operated in FM Mode. The recording was then played back at 3.75 ips and the tape recorder output was connected to a Brush Instrument Model BL-202 Oscillograph through a d.c. amplifier. The oscillograph was operated at 125 mm/second allowing the pulses to be re-recorded with a greatly expanded scale so that an accurate measurement of distance between pulses on the oscillogram could be made, which corresponded to a measurement of time. With the playback at 1/10 real-time speed and the oscillograph at 125 mm per sec, a scale of 0.0008 sec/mm was established. However, it was recognized that mechanical recorders might not always run exactly "on speed". In order to provide a check for any speed variation in the recording-playback link, a sinusoidal time-reference signal from a General Radio 1309A Oscillator was recorded on the second channel of the magnetic-tape recorder simultaneously with recording of the velocimeter output on the first channel. This reference signal was then recorded on the second channel of the oscillograph while the velocimeter pulses were recorded on the first channel. The resulting oscillogram was completely independent of any recording or playback speed variations. It was necessary, however, to insure that the known reference signal was set properly for recording and that the period of the reference

signal on the oscillogram be measured for each interval between pulses. Since the recording equipment was high quality it was decided to sacrifice some flexibility in the interest of computational convenience and assume that the recording-playback speed during the fall of a sphere could be approximated with sufficient accuracy by an average speed for that oscillogram. Thus, instead of correcting the time for each interval transit with its own unique correction factor, a time correction factor common to the entire oscillogram was applied. As a further computational convenience, a unique time reference signal was assigned for each sphere used in the investigation. This allowed identification of a particular sphere for an oscillogram by measuring the period of the reference signal.

Since the computations in this study would soon become unmanageable, a program for handling the sphere data by an IBM 360/67 digital computer was written and is listed in Appendix A. Ideally the data would have been processed by playing the magnetic-tape recording into the analog-computer section of a hybrid-computer system such as the SDS 9300/COMCOR 5000 system. The analog computer's logic could have been employed to count time between pulses and pass the information into the digital computer for real time computation of velocities, drag coefficients, and Reynolds numbers. The digital computer program given in Appendix A was originally written with hybrid operation in mind but the analog logic was not completed, in time.

The digital computer program inputs for each oscillogram corresponding to one fall of a sphere were: 1) eleven pulse interval measurements in millimeters, 2) eleven reference signal periods in millimeters, 3) fluid density in kg/m^3, 4) shear viscosity of the fluid in poise

corrected for temperature, 5) first run number for the batch of oscillograms being processed, and 6) any runs suspected of containing errors and which should not be used in computing averages of drag coefficients and Reynolds numbers.

The program contained information for each sphere and upon processing the reference signal information the information for the proper sphere was selected and used with a calculated average velocity in computing the drag coefficients and Reynolds number for that sphere for that run. The program also contained the interval distances between each pair of light planes which had been calculated from numerous measurements to assure precision in this critical part of the velocity determination. When several runs for a sphere were processed together, averages for drag coefficients and Reynolds numbers for that sphere were also calculated. As an aid to data analysis the punched data cards were returned to the computer with a program which caused a velocity history, plot of velocity for each velocimeter interval, to be printed. This allowed visual assessment of whether or not a sphere attained terminal velocity during its fall as well as detection of any unusual velocity behavior during the fall.

3. Experimental Procedure

3.1 Apparatus. The optical velocimeter was installed in the drop tank and its associated equipment connected as shown in Figs. 2.6 and 3.1. The sphere ejector was mounted on a heavy steel cantilever support above the tank as shown in Fig. 2.2. The solenoid which activated the air valve of the sphere ejector was actuated by a multiple contact switch which also connected the time reference signal to the magnetic tape recorder. This served as a convenience for finding the pulses on the magnetic tape. A portable air compressor capable of delivering small air-flow rates at pressures up to approximately 145 psi was used as a source for the sphere ejector. The regulator and accumulator allowed setting any desired pressure for sphere ejection. Since the phosphor bronze "claws" held the spheres quite firmly a minimum "break out" pressure was necessary to release the sphere from the holder. Thus it was not possible to utilize pressures much less than about 10-15 psi which, in some cases, led to initial sphere velocities considerably in excess of the desired terminal velocity.

The distance between light planes was measured by suspending a tethered 3" aluminum sphere over a pulley into the drop tank filled with water. The pulley was placed so that the sphere could be lowered into the tank along essentially the same path it would take were it catapulted from the ejector. The tether was marked and moved along a meter stick so that as the sphere was lowered into the tank the depth of the sphere could be measured with reasonable accuracy. As the sphere passed through a light plane the velocimeter

output pulse was displayed on an oscilloscope allowing the sphere to be positioned for each light plane at that point at which maximum light was reflected into the light receiver. The depth of the sphere corresponding to the "center" of each light plane was determined and the difference in depth from one plane to the next was taken as the interval distance. Several sets of determinations were made in order to obtain reasonable assurance that these critical parameters given in Table 3.1 were properly precise. Sphere ejector performance was evaluated in order to ascertain proper ejector pressure for the spheres to attain terminal velocity. Sphere number one was ejected in water at various pressures and the mean velocities within the first interval of the velocimeter were calculated as shown in Fig. 3.2.

3.2 Procedures

3.2.1. General. For the drag-coefficient determinations the ejector pressure was set to the appropriate pressure which would cause the sphere to quickly attain its "water" terminal velocity. Pressure adjustments could be made from one set of runs to the next if necessary.

3.2.2. Tests in Water. To develop confidence in the techniques employed in this study, drag coefficients of the spheres falling in water were determined and comparison with accepted values was made. The weight in air and diameter of each sphere was determined, the density was calculated, and the results, shown in Table 2.1 were incorporated in the digital computer program. Before beginning a set of runs all electronics equipment was allowed ample warm-up time, but high voltage was not applied to the multiplier phototube. A sphere was loaded into the ejector and the proper pressure was set

as described above. The high voltage to the multiplier phototube and the lamps were turned on. A few seconds delay was allowed, to insure the decay of transients in the cathode follower circuit due to the application of high voltage and light. The tape recorder, operated in FM mode, was placed in "record" and allowed to accelerate to "on speed" at 37.5 ips. The ejector switch was actuated causing the sphere to be ejected and the reference signal to be connected to the tape recorder. The recorder was stopped and lamps and high voltage turned off. Upon completion of several runs the fluid temperature was measured and recorded. The tape was then rewound and played back at 3.75 ips, the output recorded on an oscillograph, and the data analysis completed as described previously.

3.2.3. Tests in Poly(ethylene oxide) Solutions. Sphere drag coefficient determination in very dilute PEO solutions was carried out in the same manner as that for water except, of course, fluid preparation provided a greater challenge.

3.2.4. Mixing Solutions. Although POLYOX resin was water soluble, it could not be dissolved in water in the same manner as an inorganic salt. Because of the tendency for the surface of a particle to become soft and sticky in the presence of water, if the resin particles were not dispersed prior to contact with water they tended to form a gel-like agglomeration which could only be dissolved after a very extended period of time. In order to dissolve PEO resins in water, Union Carbide Chemicals Company (59) recommended pre-dispersion be accomplished either by mechanical means or by taking advantage of the insolubility of PEO resins in various liquids. In the latter case boiling water could even be used as the dispersion

carrier due to the inverse temperature - solubility property of PEO. Of more practical use, however, was the use of a polypropylene glycol for the dispersal agent as was done by Forester and Francis (10) during friction reduction tests for the David Taylor Model Basin and by McClanahan and Ridgely (27). The polypropylene glycol used in their tests was of molecular weight about 400 and was marketed by Dow Chemical Company as POLYGLCOL P400. PEO was completely insoluble in POLYGLYCOL but the POLYGLYCOL was miscible with water allowing the resulting dispersion to be injected into water so that the PEO could be readily dissolved. Of significance is the observation made by Forester and Francis that the dispersion carrier produced no drag reduction when injected alone into water. Thus, any drag reduction observed was due to the PEO and not the polypropylene glycol. For this investigation PEO concentration of 1000, 200, and 100 wppm were to be tested. A slurry of 1.081 Kg of PEO suspended into 2 Kg of POLYGLYCOL was prepared. This slurry, when dispersed into the drop tank containing 1081 Kg of fluid when filled with tap water to within 0.1 m from the top, yielded an aqueous solution of 1000 wppm poly(ethylene oxide). After the dispersion was completely emptied into the tank and the tank was filled to the proper level the solution was stirred gently for 18 hours with two Cole-Parmer mixers operated at very slow speed to insure complete solution of the resin without undue polymer degrading turbulence and to provide some assurance of homogeneity of the solution. For tests with 200 wppm a slurry of 0.216 Kg PEO in POLYGLYCOL was prepared and emptied slowly into the tank while it was being filled with tap water. Gentle stirring by both mixers was

carried out during the entire time the slurry was emptying into the tank as well as for about two hours afterward when the PEO resin appeared to be completely dissolved. The 100 wppm PEO was prepared by draining the 200 wppm solution from the tank to a fluid level 0.936 m below the tank top, refilling with tap water, and stirring.

It has been reported by McGary as well as other investigators that several ions often present in tap water cause degradation in POLYOX. A typical analysis of the water used is given in Table 3.2 in order that some assurance be given that no significant degradation due to chemical action affecting drag reduction would result.

After the solution was prepared sphere drag coefficients were determined as was done for water. For each concentration samples of the fluid were taken at several levels in the tank and capillary tube viscosity determinations were made. This allowed obtaining information as to the actual homogeneity of the fluid as well as to determining intrinsic viscosity of the POLYOX resin. The molecular weight of the PEO resin used was estimated using the expression given by Shin (46) relating intrinsic viscosity to molecular weight for $25^{o}C$:

$$[r] = 1.03 \times 10^{-4} M^{0.78}$$

4. Results and Discussion

4.1. Drag Coefficients in Water and Dilute Poly(ethylene oxide) Solutions. The results of the sphere drag-coefficient determinations in water, 1000 wppm PEO, 200 wppm PEO, and 100 wppm PEO are presented in Fig. 4.1, 4.2, 4.3 and 4.4 respectively. Since no significant data display improvement would have resulted by pretending that the solution shear viscosity obtained by capillary-tube viscometry had meaning, drag coefficients were plotted with water Reynolds numbers instead of solution Reynolds numbers. This was done as a matter of convenience for comparing these data with the results obtained by other investigations. Except for the 1000 wppm solution, the resulting solution Reynolds numbers would have differed from the water Reynolds numbers by a barely perceptible amount. The use of the generalized Reynolds numbers for power law fluids suggested by Dodge and Metzner (8) would not have resulted in an improved data display.

The wind-tunnel data for spheres attributed to Weiselsburger as presented by Schlicting (43) are shown as a solid curve on all the graphs.

It is significant that the sudden drop in drag coefficient associated with the drag crisis observed for spheres moving in air and water was also observed at about the same Reynolds number for all PEO solutions investigated. However, the values of drag coefficients for Reynolds number less than the critical value, as well as those slightly greater, were considerably lower than for water and air. Data at the lower limit of Reynolds numbers for this investigation coincided with results reported by Lang and Patrick at the upper Reynolds number limit of their investigation.

Another significant observation is that when the Reynolds number is increased above the critical value, the drag coefficient returns precipitously to nearly the same value as for water. This feature could not be further defined since it occurred at the upper limit of Reynolds numbers for this investigation, about 8×10^5. In the region above the critical Reynolds number a very slight PEO concentration dependence was observed with the 1000 wppm producing greatest drag reduction and 100 wppm producing least drag reduction.

Sphere size did not affect drag reduction if the water Reynolds number was equal. It is seen that the 2 1/2 inch brass sphere and 4 inch aluminum sphere had approximately the same drag coefficient at a Reynolds number of about 6×10^5 in 1000 wppm PEO.

4.2. Sphere Behavior During Fall. During the fall of some spheres, deviation from the vertical path, either curvature or occassional spiralling was observed. For a given sphere in a particular fluid the deviation seemed to be the same from one fall to the next. The maximum eccentricity of the spheres was 0.2% and this was not a contributing factor. The sphere holder on the ejector was readjusted and the same deviation occurred. All spheres fell more smoothly and had more nearly vertical paths in 1000 wppm PEO. The velocity correction would have been only about 1.03 for a sphere moving along a straight path from the tank center at the top to the tank side at the bottom. However, those runs in which the sphere deviated widely from the vertical path were excluded from the data presented here. The brass spheres, almost without exception, fell in vertical paths.

As had been anticipated (see Fig. 2.1) the 3 inch aluminum sphere, (number 8), yielded two values of drag coefficients. Other spheres had been expected to yield multiple results but sphere 8 was the only one tested specifically for this effect. The upper value of drag coefficient (see Figs. 4.1 and 4.2) was obtained by setting the sphere ejector for minimum ejection speed and the lower values by selecting a higher ejection speed. A phenomenon of interest was observed in the speed histories. In the first cases the sphere decelerated to its terminal speed. For the lower drag coefficients, the sphere accelerated and settled to its terminal speed with no observable oscillation. Apparently, in the second case, the ejection speed had been sufficiently high to skip over the lower terminal speed. It is likely that a sphere falling from rest could not have made this "jump", although no supporting evidence for this was obtained. This phenomenon is not related to the dual terminal velocity behavior for some spheres reported by Sanders (42) since the present phenomenon was predictable on the basis of the shape of the drag coefficient curve whereas that reported by Sanders apparently resulted from another mechanism characteristic of the fluid.

The paucity of data presented for 200 wppm and 100 wppm PEO resulted from the exclusion of so many drops in which the spheres did not decelerate to terminal speed after having been ejected at a much too great ejection speed. This was not apparent until after data analysis began and the plots of time history for each drop were obtained from the computer. Had these histories been available sooner it might have been feasible to repeat many drops with more appropriate

ejection speeds. Nevertheless, even with so few data, the general trend indicated by the 1000 wppm data, can be observed in the 200 wppm and 100 wppm data.

4.3. Degradation of Poly(ethylene oxide). No degradation resulting from the spheres falling in the PEO solutions could be determined. Intrinsic viscosity determinations by capillary tube viscometry, before and after a days run produced no measurable change in the value of intrinsic viscosity from the initially measured value of 8.6 $\pm$ 1.0 deciliters/gram at 25^{o}C and thus probably no change in molecular weight. In addition, the shear viscosity of 200 wppm solution samples changed from 1.13 centipoise at 25^{o}C within a few hours after mixing to 1.12 centipoise at 25^{o}C ten days later. This indicated that the likelihood of degradation due to ageing during the sphere drops conducted within 24 hours after mixing was very small.

The expression given by Shin (46) for PEO molecular weight and intrinsic viscosity at 25^{o}C was used to calculate the molecular weight of the PEO WSR 301. The resulting value of 2.0×10^{6} is approximately half that given by the manufacturer. The resin used had been stored in its unsealed paper carton for approximately 2 1/2 years prior to this investigation. Polymer resin degradation cannot be proven on the basis of this determination alone since no molecular-weight determination for the new resin was available. Since, Pruit, Rosen, and Crawford (38) obtained a value of 1.57×10^{6} for WSR 301 there may be no problem here at all.

5. Conclusions

5.1 Drag Coefficients of Spheres. The effect of the addition of poly(ethylene oxide) to water on the drag of free-falling spheres is best discussed with the assistance of a plot of drag coefficients vs water Reynolds number (Fig. 5.1). The lines represent a "best" estimate of the shape of the drag coefficient curve as visually fitted to all available data. These estimates were based on the results reported by Lang and Patrick (26), Hayes (20) and Chenard (5) for Reynolds number less than 1.5×10^5 and on the results of this investigation at greater Reynolds numbers.

From results reported by previous investigators it is seen that, as Reynolds number increases above about 10^4, drag enhancement changes to drag reduction which increases with increasing Reynolds number. Furthermore, drag reduction is increased by decreasing concentration from 1000 wppm to 100 wppm.

As the critical Reynolds number is approached from below, the concentration dependence seems to become less until about 2×10^5 it is not measurable. Admittedly, this latter conclusion is based on a minimum of data but, because of the very great difficulty in obtaining free-fall data at the critical Reynolds number, it is not likely that the curve will be better defined unless experimental technique superior to those used in the past are developed. Nevertheless, the results of this investigation show that at just above 2×10^5 there is no measurable concentration dependence for sphere drag coefficients in 1000 wppm and 200 wppm PEO solutions. The estimated curve from this point until Reynolds numbers above the critical value are reached is a guess since there is no data, except for the end points, to support the curve shape estimate during the drag crisis.

In the Reynolds number region between 3×10^5 and about 7×10^5, there is a very small polymer concentration dependence with 1000 wppm PEO solutions giving greatest drag reduction and 100 wppm solutions the least.

An abrupt rise occurs above 7×10^5 which suggests a behavior similar to that of cylinders as measured by Roshko (40) and shown in Fig. 5.2. This lends further support to the speculation by Sanders (42) as to the applicability of Roshko's laminar separation bubble to flows about spheres. If this speculation has any basis, then the drag reduction experienced in the Reynolds number region between 3×10^5 and 8×10^5, called the supercritical region by Roshko, is characterized by the effect of the polymer on the laminar separation bubble. This explanation of polymer effect in the supercritical region is consistent with the mechanism proposed by Sanders (42) for subcritical Reynolds numbers. In both cases the polymer effect is restricted to altering the character of the laminar boundary layer.

At a Reynolds number of about 8×10^5, drag coefficients in all fluids tested in this investigation(including water) were of nearly the same value. This apparent equality of drag coefficients may be indicative of turbulent boundary layer separation and, further, indicative that the turbulent boundary layer is unaffected by polymer concentration.

As indicated in Fig. 5.1 the use of the virtual mass coefficient, $K_1 = 1.8$, for separated laminar boundary layer flows past spheres, as was done by Lang and Patrick (26), Hayes (20), and Chenard (5), was corroborated. No such support was given, however, for the use of $K_1 = 0.5$ for separated turbulent boundary layer flows as used by Chenard.

Sphere size had no effect on drag reduction in PEO solutions at a water Reynolds number of 6×10^5.

5.2 Drag Coefficients of Free-falling Spheres in Water. Reference to Fig. 4.1 shows that below drag crisis the drag coefficients obtained in water agree more closely with the results of Lunnon's investigations of free-falling spheres (see Goldstein 15) than they do with Weiselsberger's wind tunnel data. On the other hand, beyond drag crisis the drag coefficients are still slightly greater than those reported by Weiselsberger but much less than those reported by Bacon and Reid (2). It has long been thought that, for free-falling spheres, the Lunnon curve could be extrapolated across the drag crisis region to join the Bacon and Reid curve. The results of the present investigation are inconsistent with this extrapolation. It appears that either the ejected spheres of this investigation did not behave strictly as free-falling spheres or that the Bacon and Reid results cannot be valid for free-falling spheres in the super-critical region. It may be that some slight turbulence in the drop tank may have altered the fall in some way but it is obvious that the spheres falling in the atmosphere as investigated by Bacon and Reid must have been influenced in some similar way. Thus, it seems that beyond drag crisis good wind tunnel data, such as that of Weiselsberger, better describes the drag of free-falling spheres than does the Bacon and Reid results.

5.3 Polymer Degradation. The poly(ethylene oxide) solutions did not measurably degrade during the sphere drops nor was degradation due to

aging of a 200 wppm solution observed within 10 days after the solution was mixed.

5.4 Comments on the Experiment. The technique of ejecting spheres vertically at or near terminal speed and measuring the vertical velocity component provided an effective means of extending the range of experiments in PEO solutions. The limiting factors were significant deviation from a vertical path by some spheres during some drops and the laborious data reduction involved in reading oscillograms and manually inserting digital data into the computer. Of more than 300 drops data analysis showed that only about 150 could be used with certainty due to erroneous selection of ejection speed. Nevertheless, if one is persistent, this technique can produce meaningful results for spheres in fluid flows at and above the critical Reynolds number of water.

TABLE 1.1

MOLECULAR WEIGHTS OF POLYOX RESINS

POLYOX Resin	Approximate Molecular Weight
WSR 35	2×10^5
WSR 205	6×10^5
WSR 301	4×10^6
Coagulant	5×10^6
WSR 701	6×10^6

TABLE 2.1

CHARACTERISTICS OF SPHERES USED FOR DRAG MEASUREMENTS

Sphere number	Material	Diameter, m	Mass, Kg	Density Kg/m^3	Estimated Fall distance for terminal velocity, m	Estimated Terminal velocity, m/sec
1	Brass	0.10132 ± 0.00022	4.584	8416.3	11.1	8.6
2	Brass	0.08886 ± 0.00010	2.921	7950.0	9.3	8.6
3	Brass	0.07598 ± 0.00011	1.826	7952.4	8.0	8.4
4	Brass	0.06350 ± 0.00014	1.131	8437.9	7.0	8.1
5	Aluminum	0.10099 ± 0.00019	1.501	2782.8	5.0	4.9
6	Aluminum	0.08876 ± 0.00019	1.016	2775.8	4.4	4.9
7	Brass	0.05058 ± 0.00003	0.573	8460.9	5.5	3.5
8	Aluminum	0.07621 ± 0.00008	0.645	2780.5	0.7	2.1
9	Aluminum	0.06347 ± 0.00014	0.361	2697.5	0.6	1.8
10	Aluminum	0.05083 ± 0.00010	0.191	2779.6	0.5	1.5

TABLE 3.1

DISTANCES BETWEEN LIGHT PLANES OF OPTICAL VELOCIMETER

Interval, I	Bounded by light planes	Distance, S(I),m
1	1 - 2	0.1078 ± 0.0064
2	2 - 3	0.1075 ± 0.0049
3	3 - 4	0.1092 ± 0.0043
4	4 - 5	0.1103 ± 0.0035
5	5 - 6	0.1101 ± 0.0029
6	6 - 7	0.1077 ± 0.0019
7	7 - 8	0.1101 ± 0.0027
8	8 - 9	0.1073 ± 0.0038
9	9 - 10	0.1109 ± 0.0034
10	10 - 11	0.1102 ± 0.0027
11	11 - 12	0.1093 ± 0.0032

TABLE 3.2

TYPICAL GRAVIMETRIC ANALYSIS OF WATER
SUPPLIED BY MONTEREY CITY WATER COMPANY

Substance	PPM	Substance	PPM
Silica	21.1	K	2.0
Iron	0.1	CO_3	99
Mn	0	Cl	13.0
Al	0	SO_4	28.0
Fl	0.25	Total dissolved solids	165
CO_2	3.1	Total $CaCo_3$	105
Ca^2	26.4	NonCarbon hardness	24
Mg	9.5	PO_4	0.05
Na	11.9	H^{+4}	7.7 pH

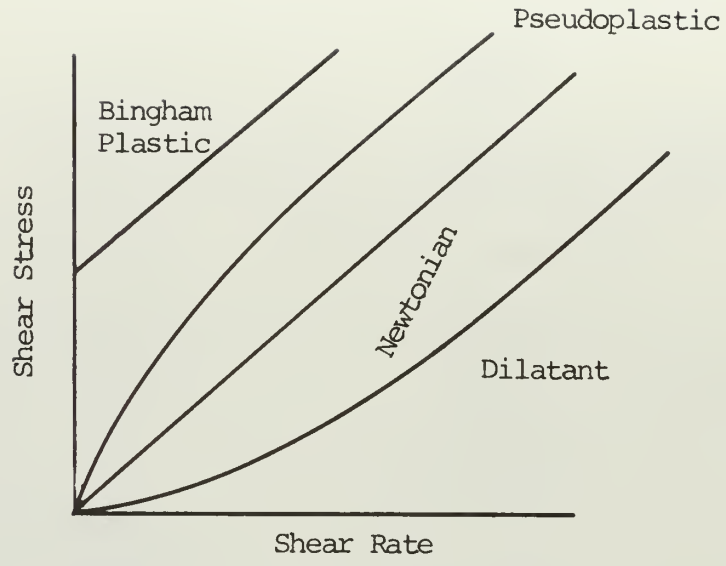

Figure 1.1 Shear Flow Curves

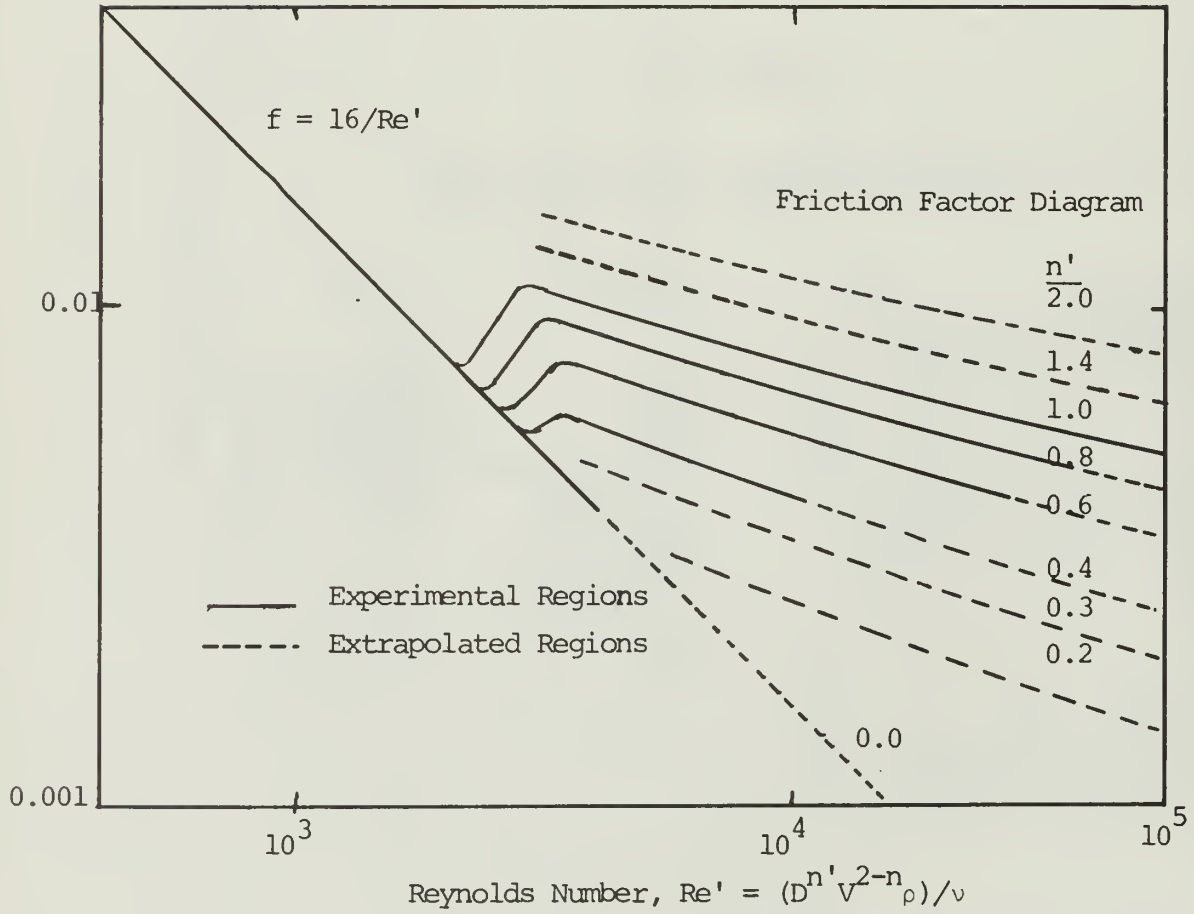

Figure 1.2 Friction Factor Design Chart for Newtonian and Non-Newtonian Fluids.

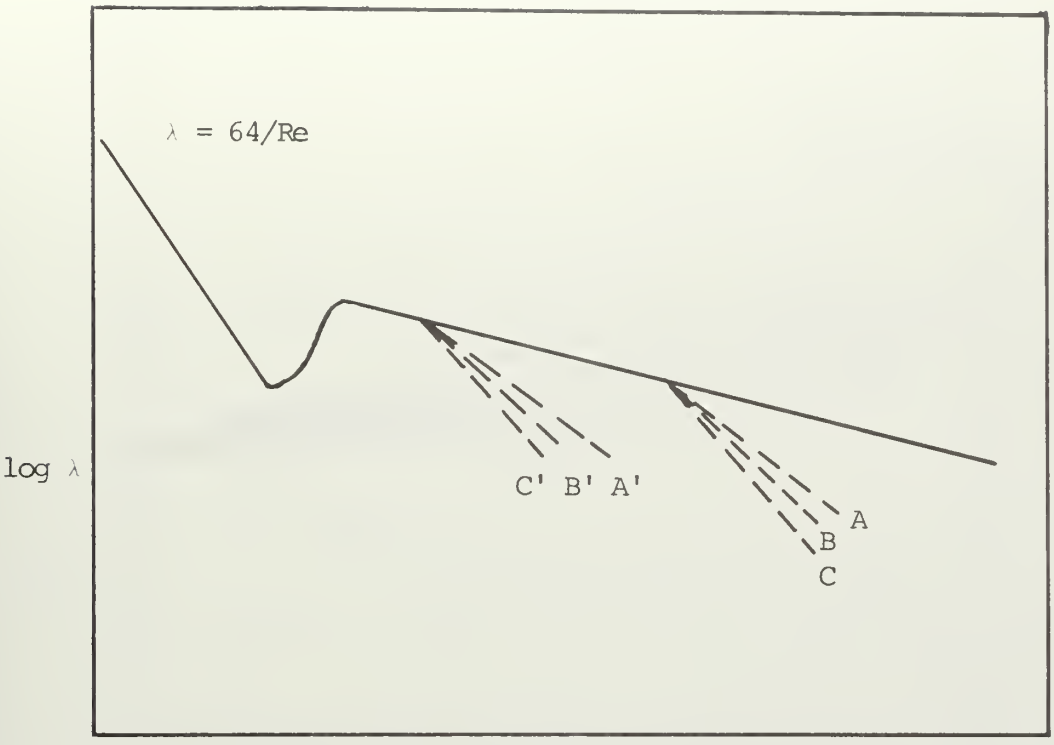

Figure 1.3 Friction Reduction in Pipes for Some Additives.

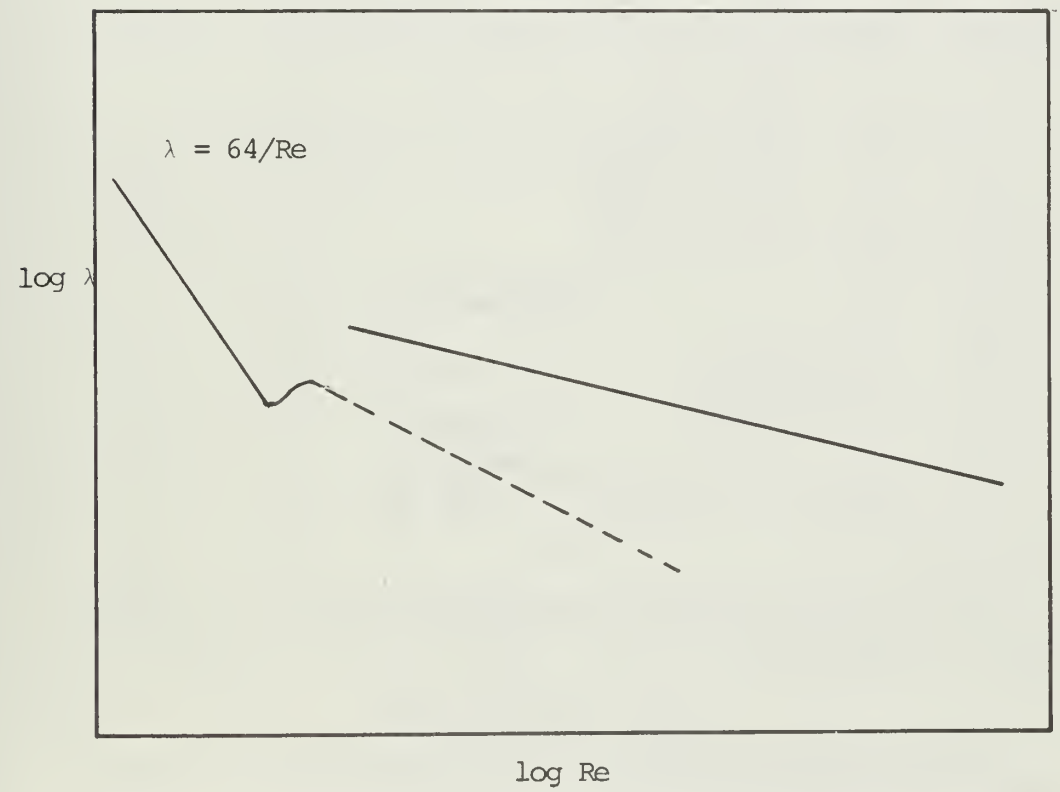

Figure 1.4 Friction Reduction in Pipes for Some Additives

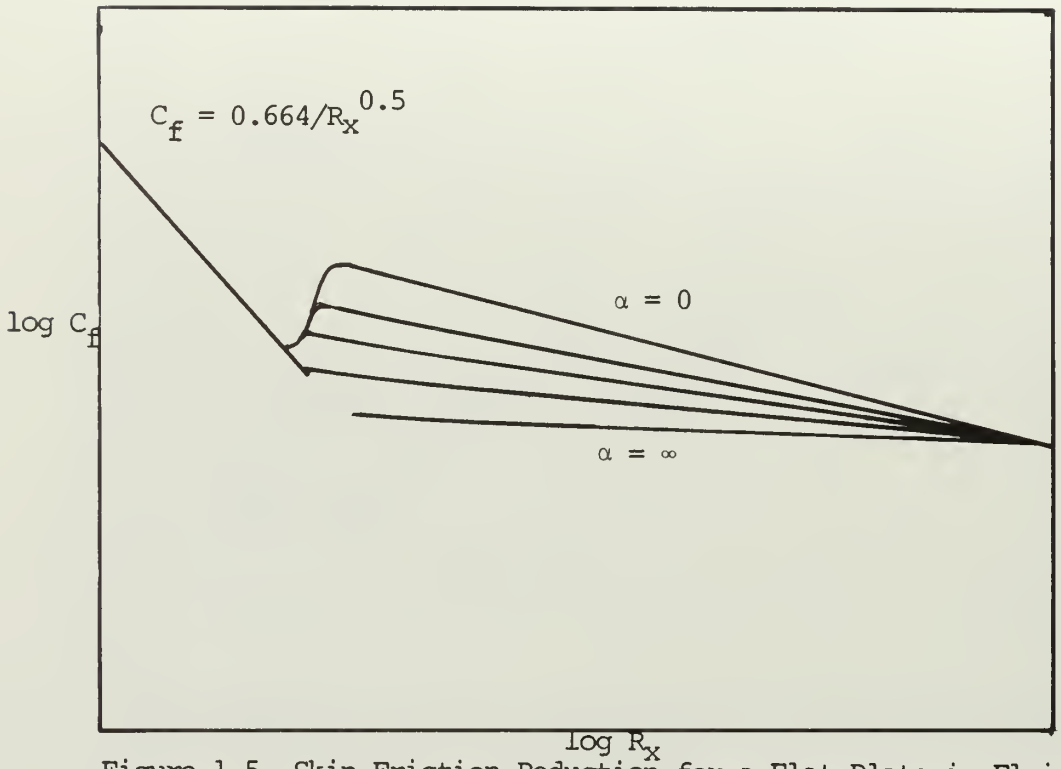

Figure 1.5 Skin Friction Reduction for a Flat Plate in Fluid Containing Polymer Additive.

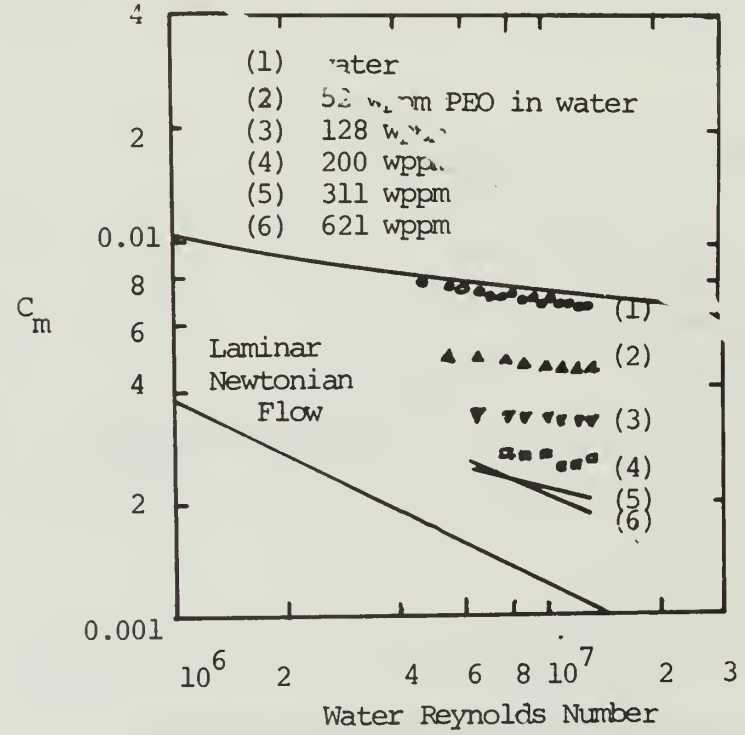

Figure 1.6 Torque Reduction for a Rotating Disk.

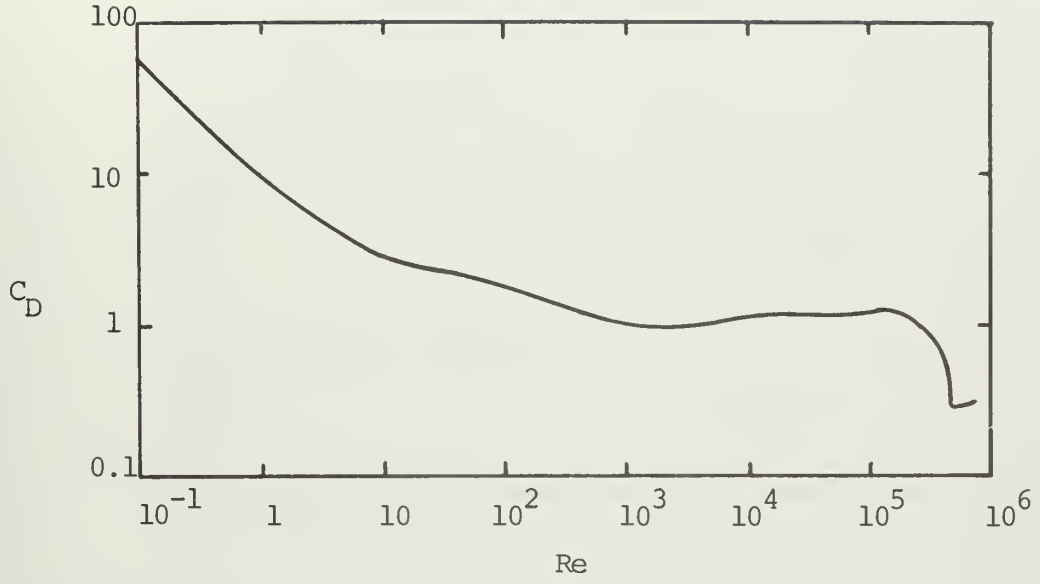

Figure 1.7 Drag Coefficients for Circular Cylinders (Weiselsberger).

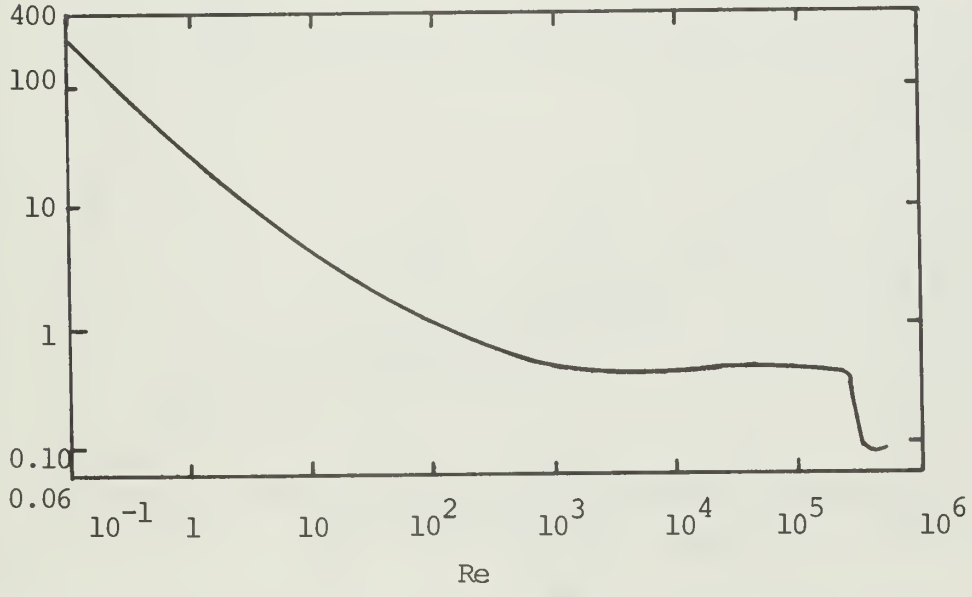

Figure 1.8 Drag Coefficients for Spheres (Weiselsberger).

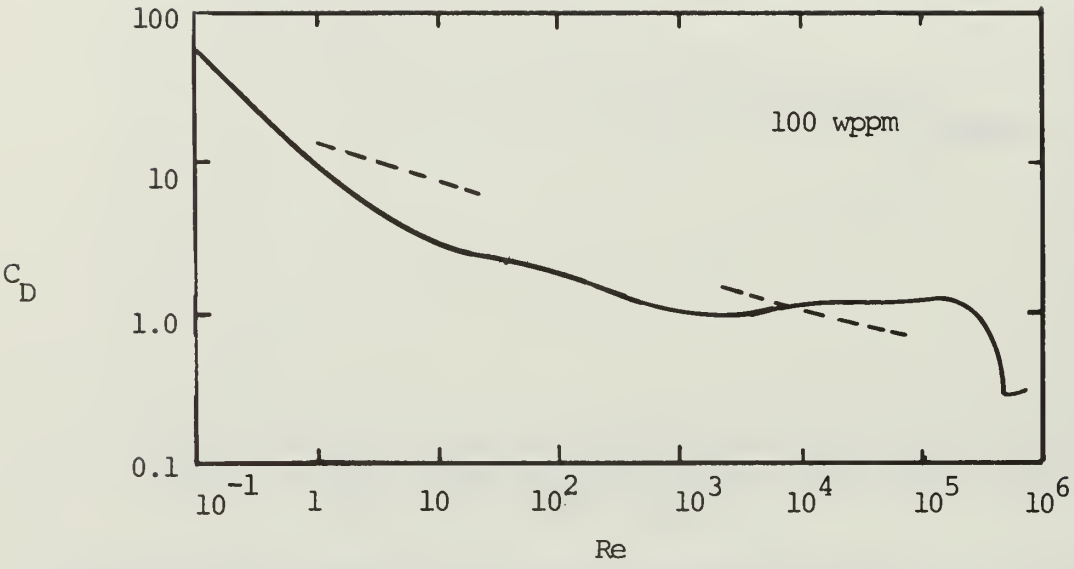

Figure 1.9 Trend of Drag Coefficients for Circular Cylinders in Dilute Aqueous PEO Solutions.

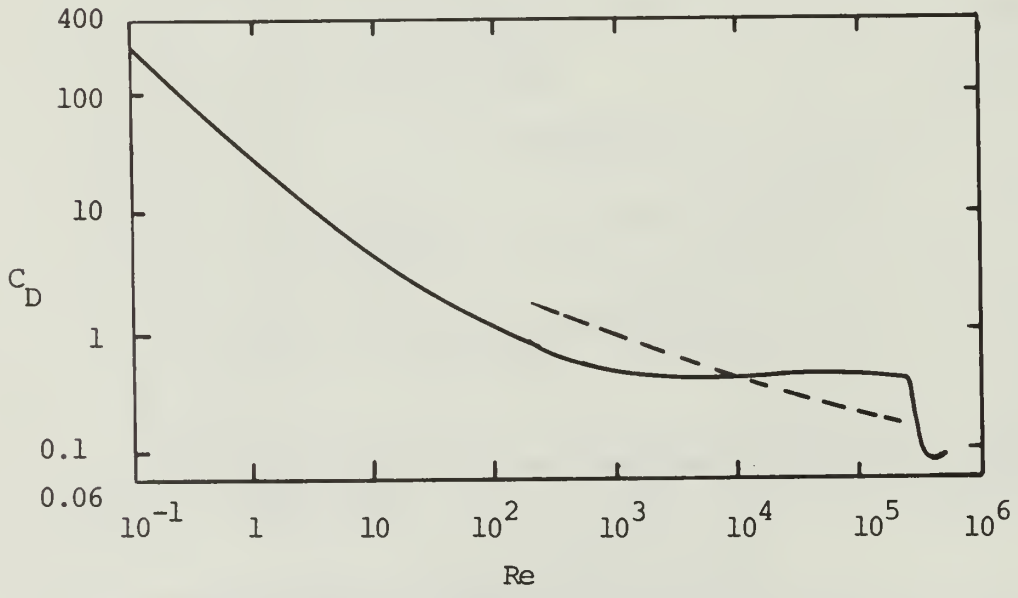

Figure 1.10 Trend of Drag Coefficients for Spheres in Dilute Aqueous PEO Solutions.

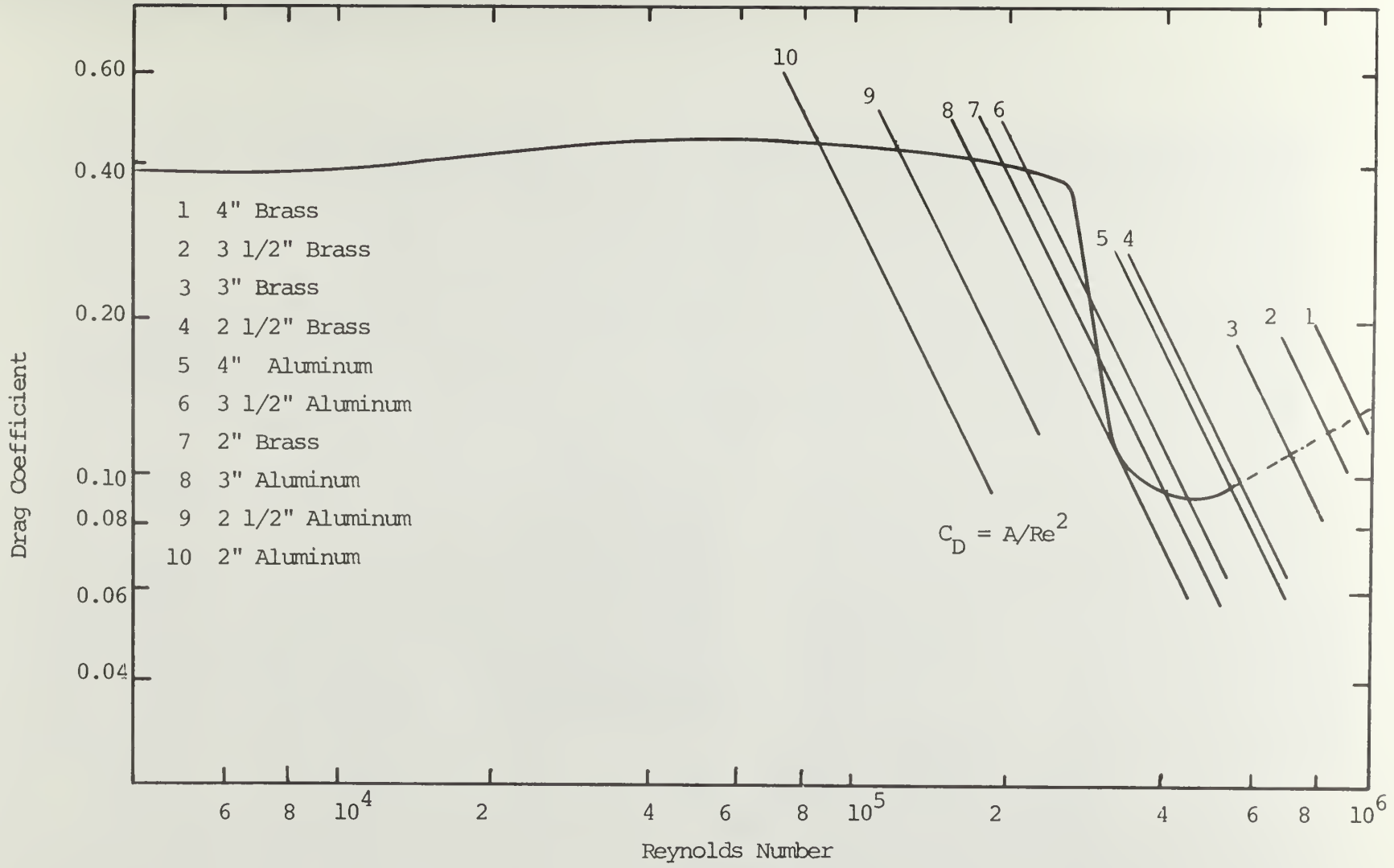

Figure 2.1 Predicted Re Ranges for Spheres of Various Sizes and Materials.

Figure 2.2 View of Top of Drop Tank with Sphere Ejector and Optical Velocimeter Installed.

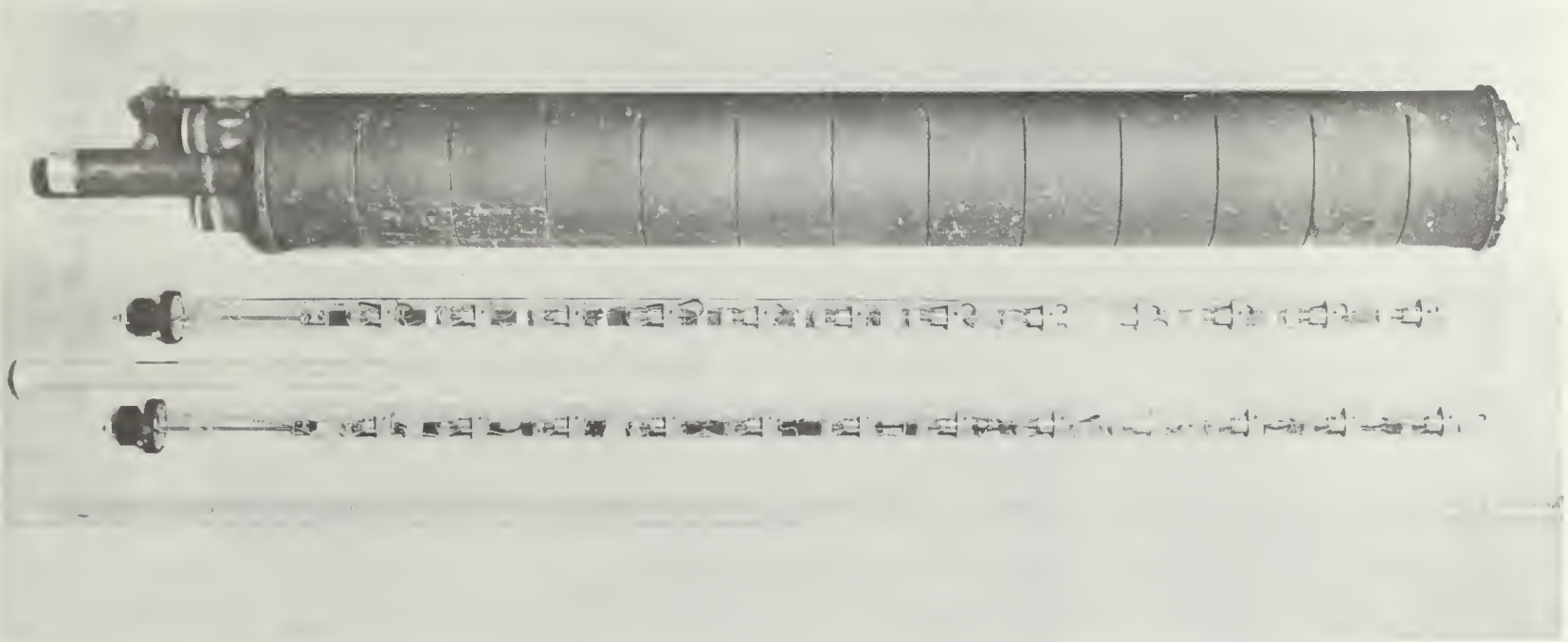

Figure 2.3 Disassembled Optical Velocimeter

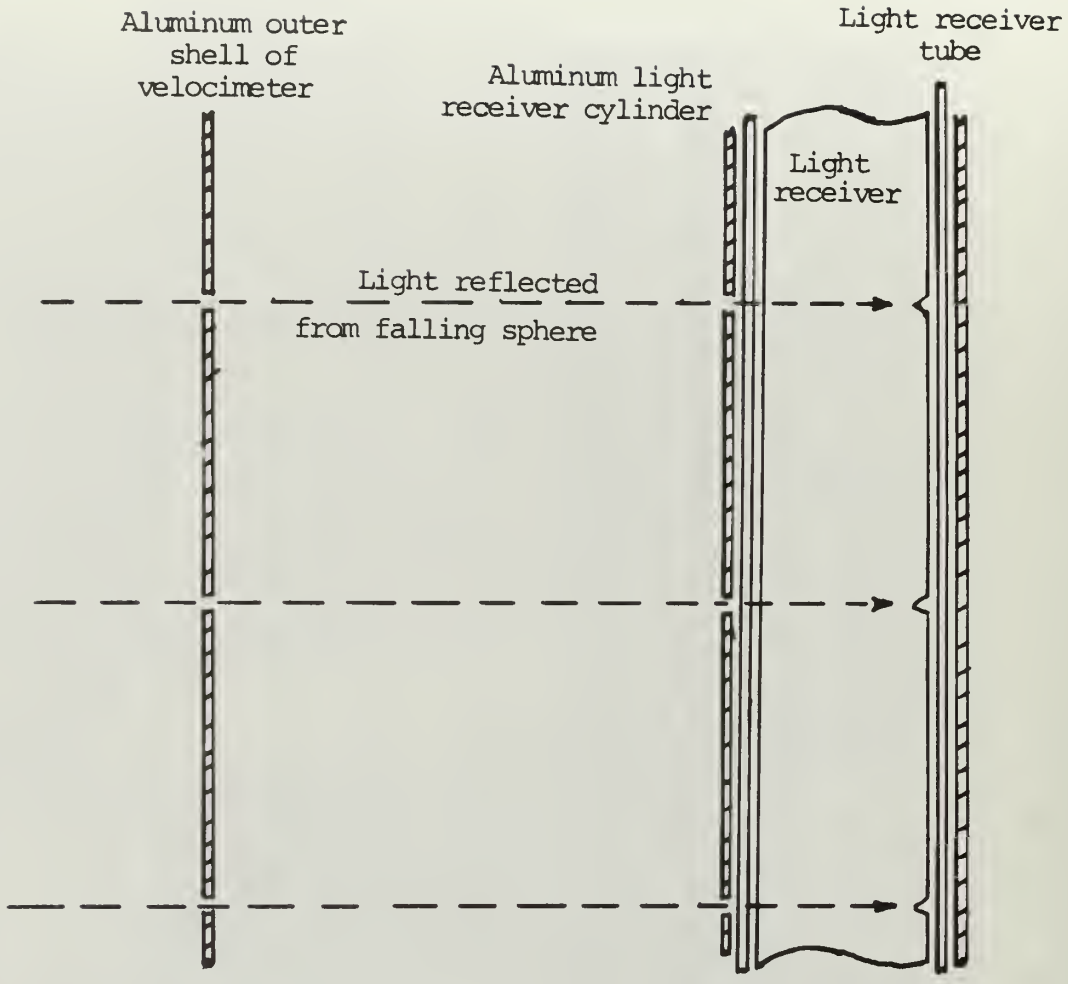

Figure 2.4 Diagram of path of light rays into light receiver.

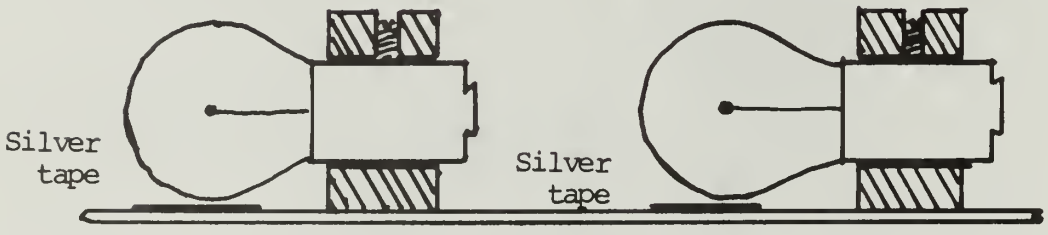

Figure 2.5 Diagram of Lamp socket mounting.

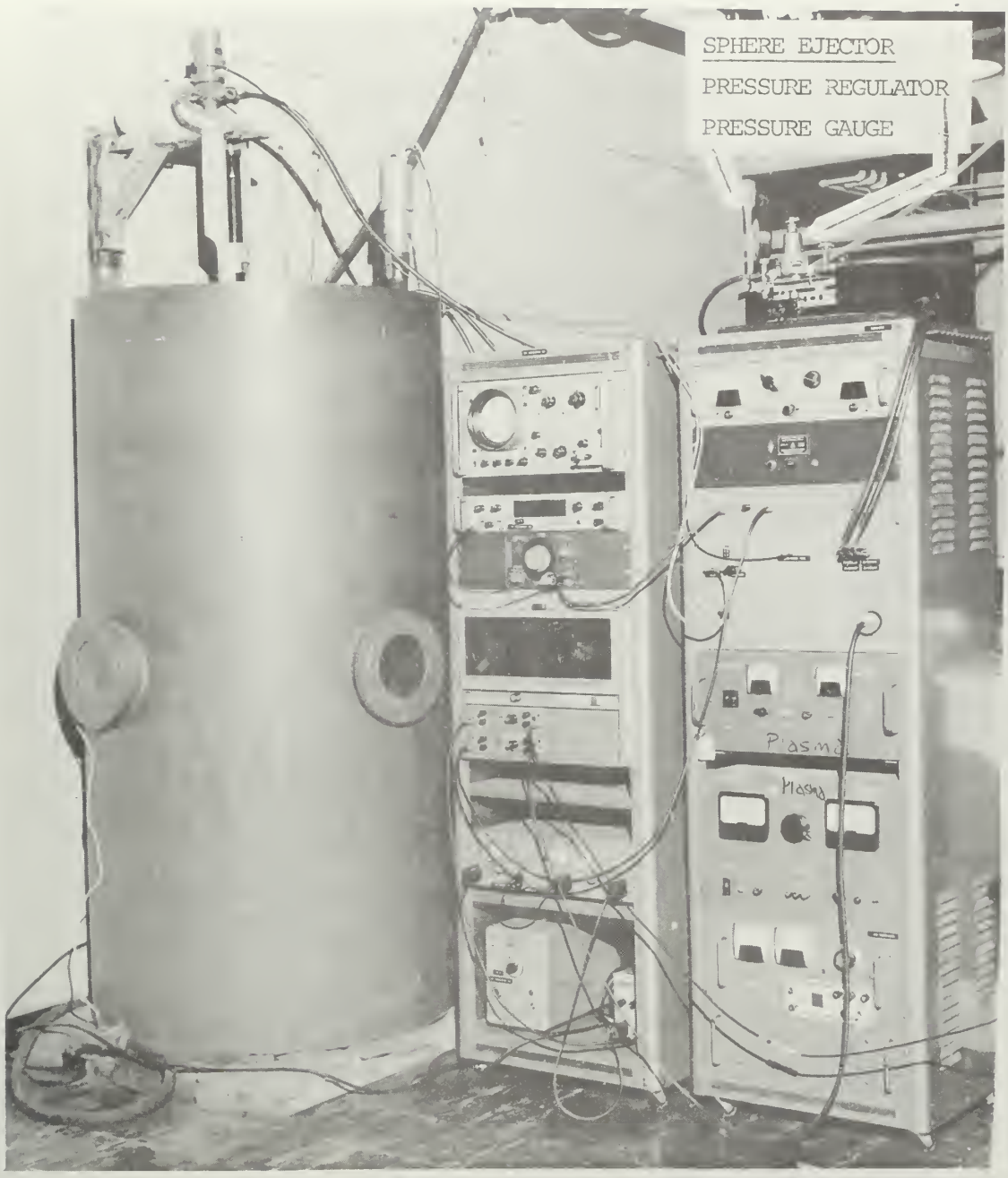

Figure 2.6 View of Apparatus Employed in Sphere Drag Measurements.

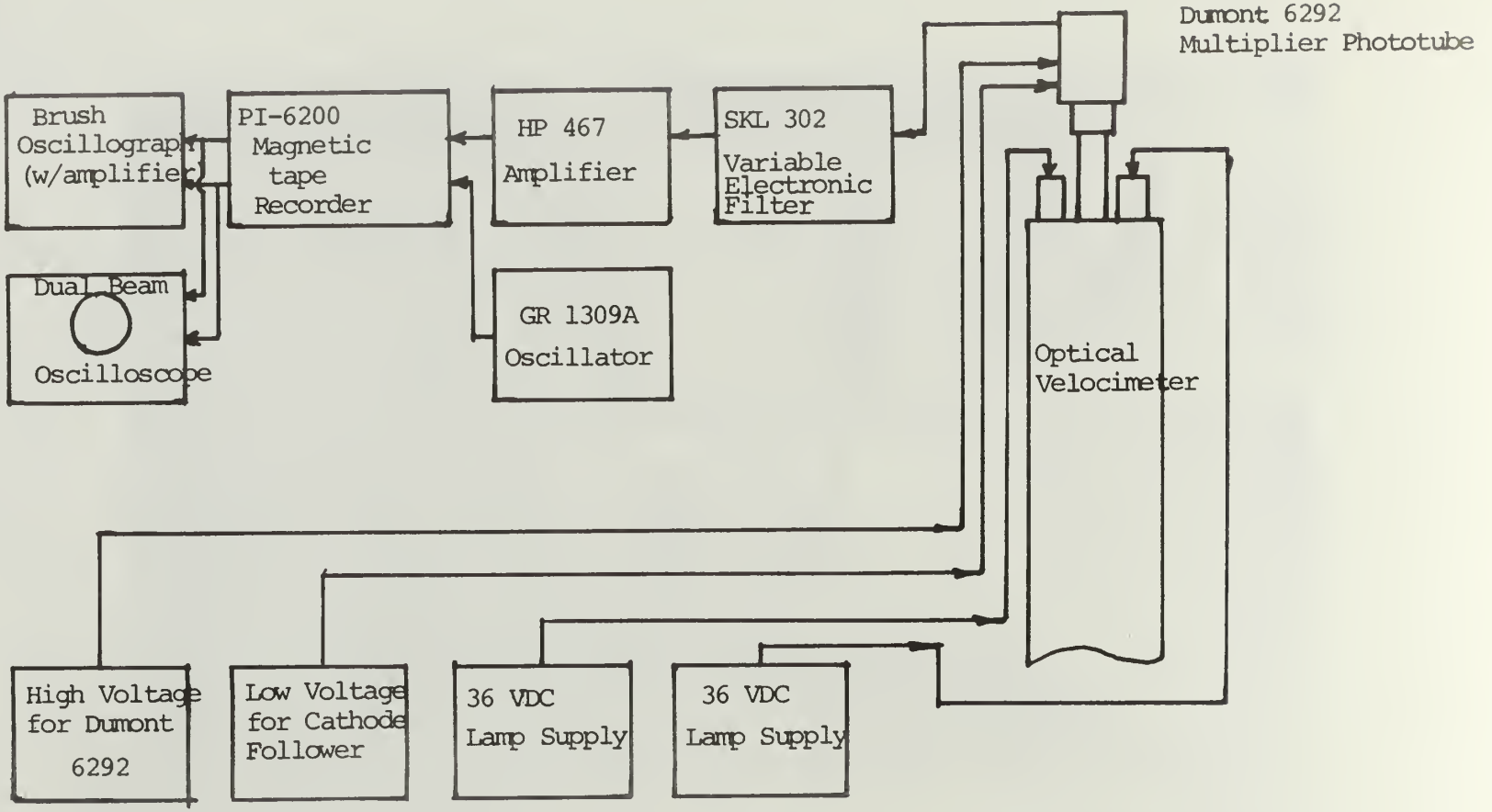

Figure 3.1 Block Diagram of Velocimeter Electrical Supplies and Electronics Equipment.

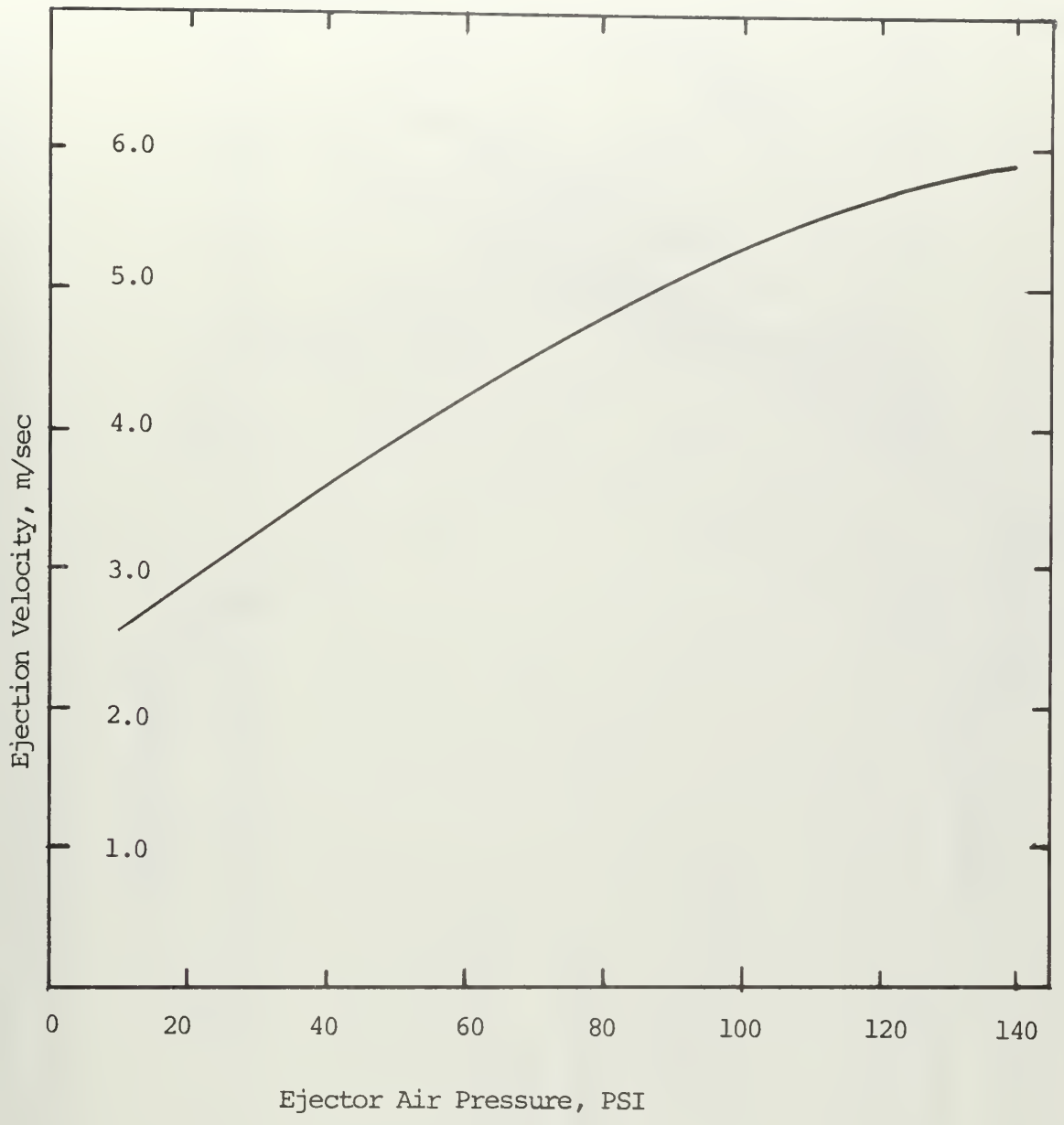

Figure 3.2 Sphere Ejector Performance with 4 Inch Brass Sphere.

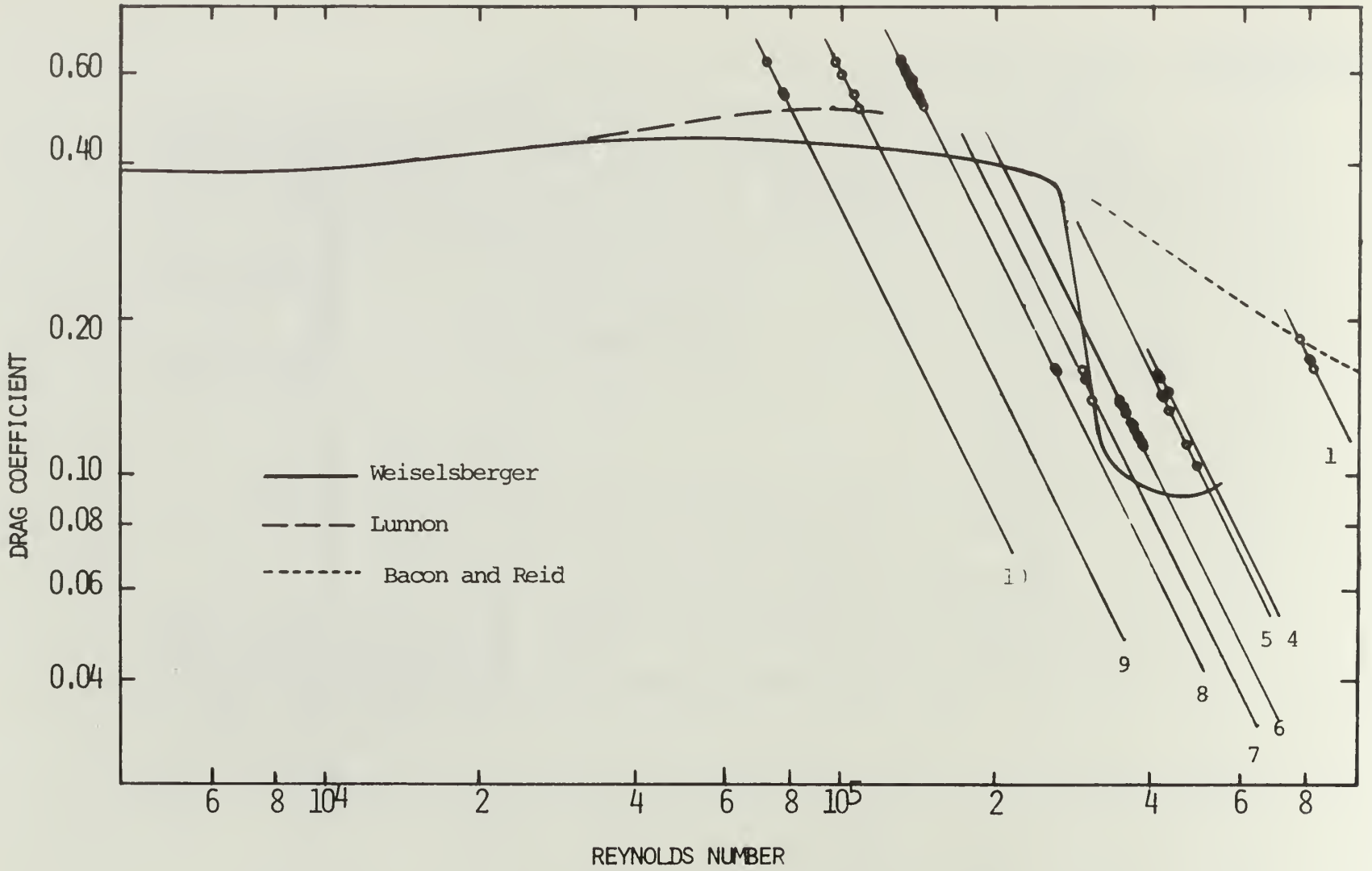

Figure 4.1 Measured Sphere Drag Coefficients in Water.

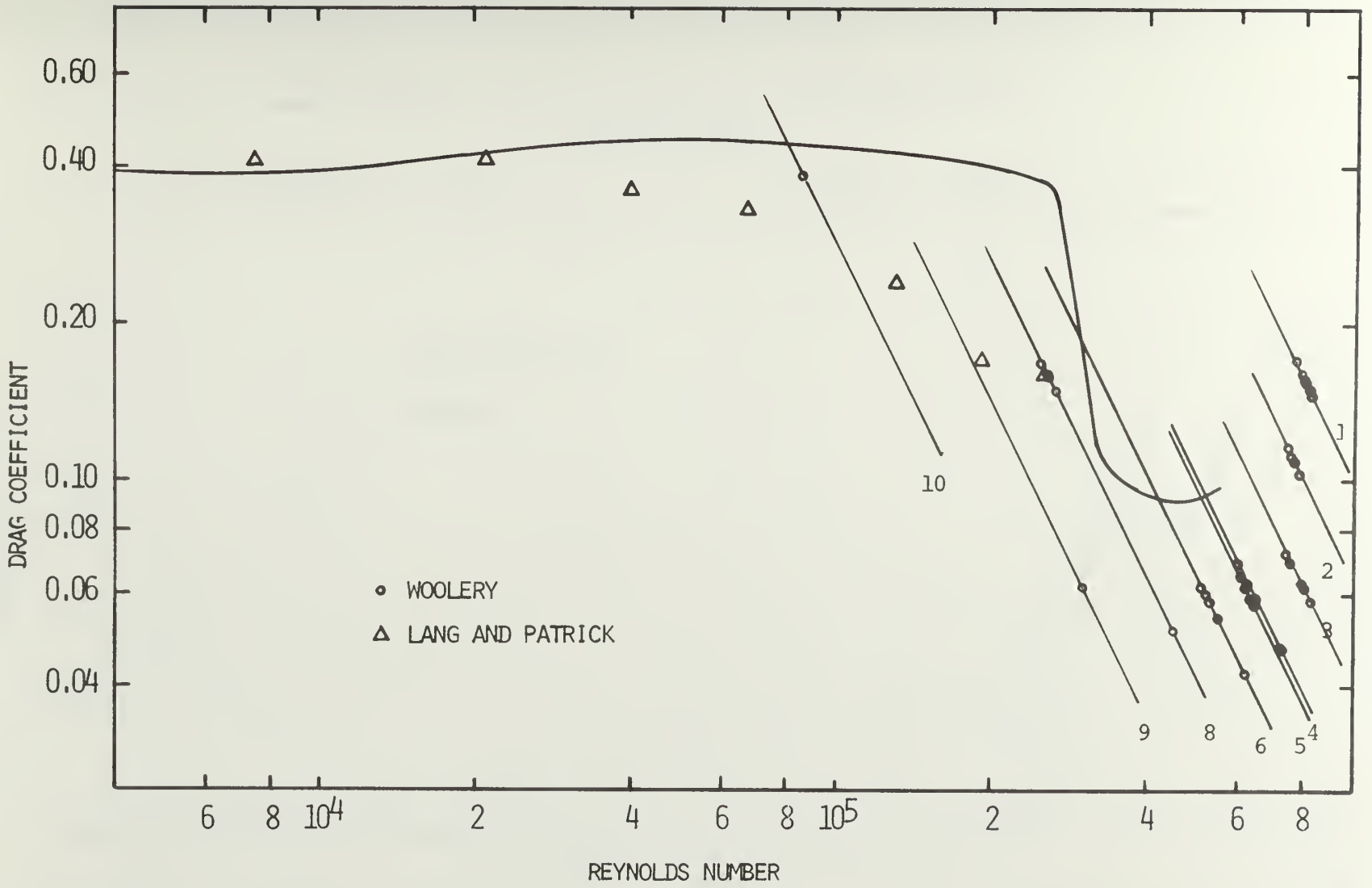

Figure 4.2 Measured Sphere Drag Coefficients in 1000 wppm PEO Solution.

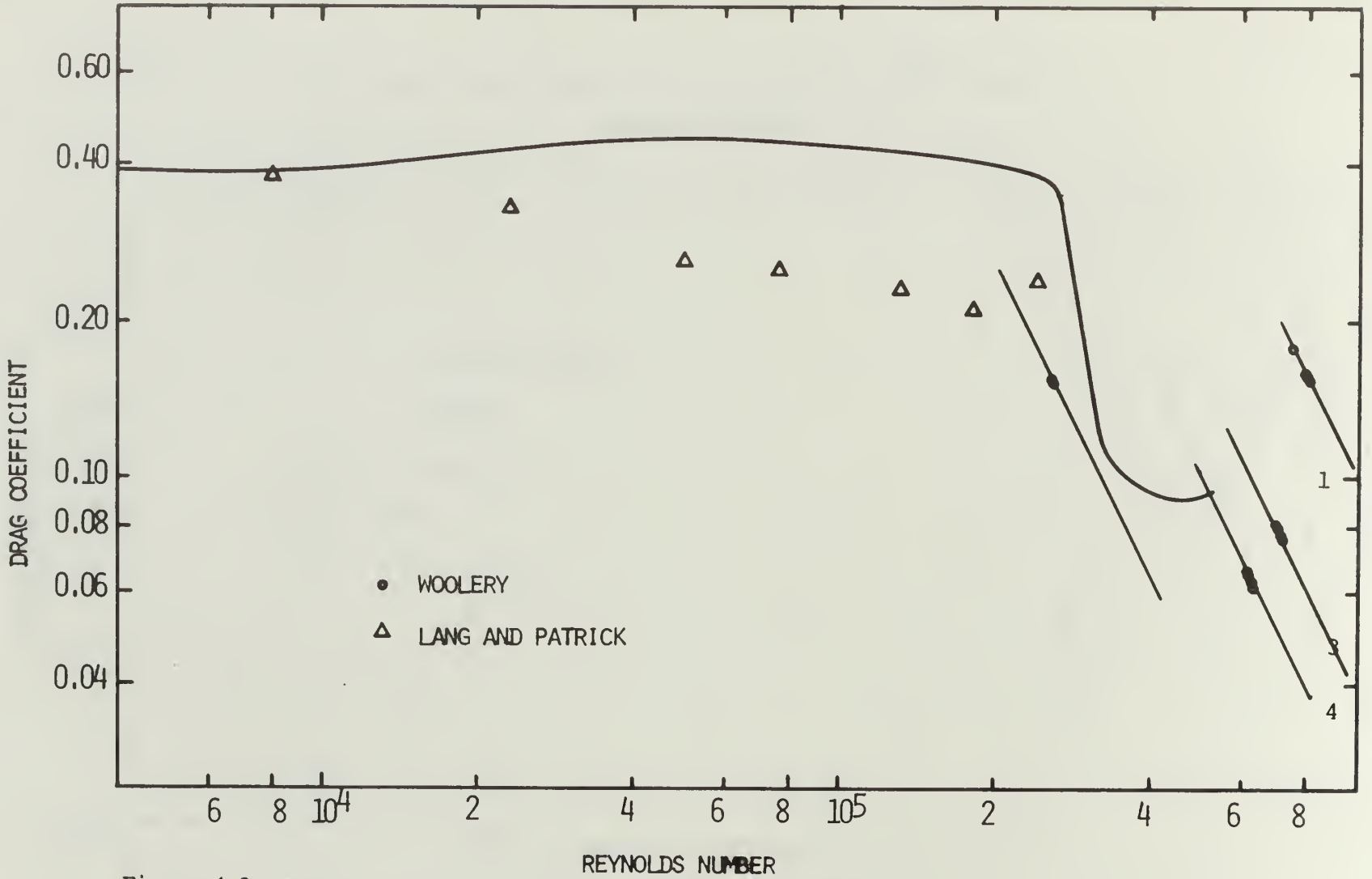

Figure 4.3 Measured Sphere Drag Coefficients in 200 wppm PEO Solution.

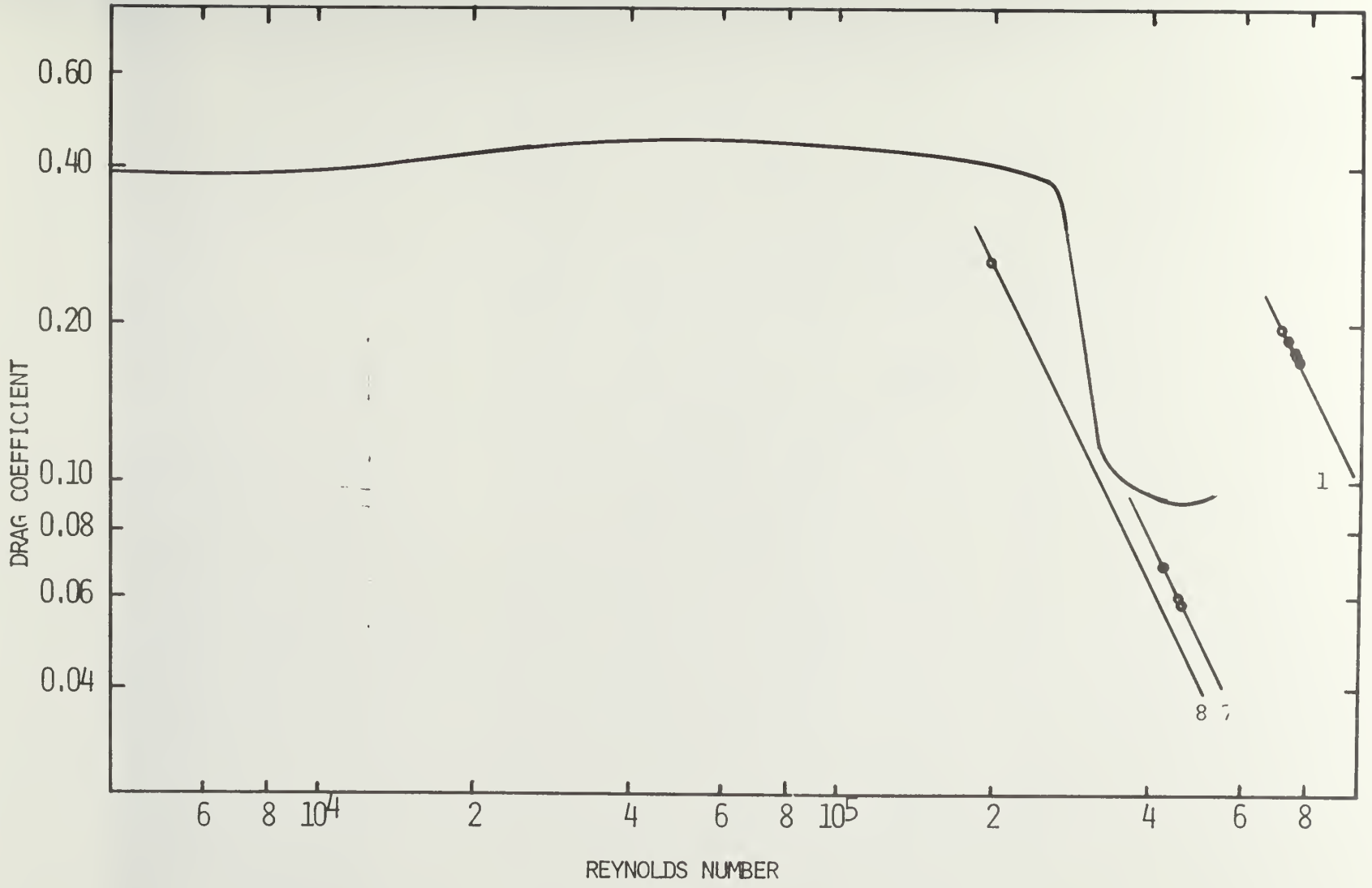

Figure 4.4 Measured Sphere Drag Coefficients in 100 wppm PEO Solution.

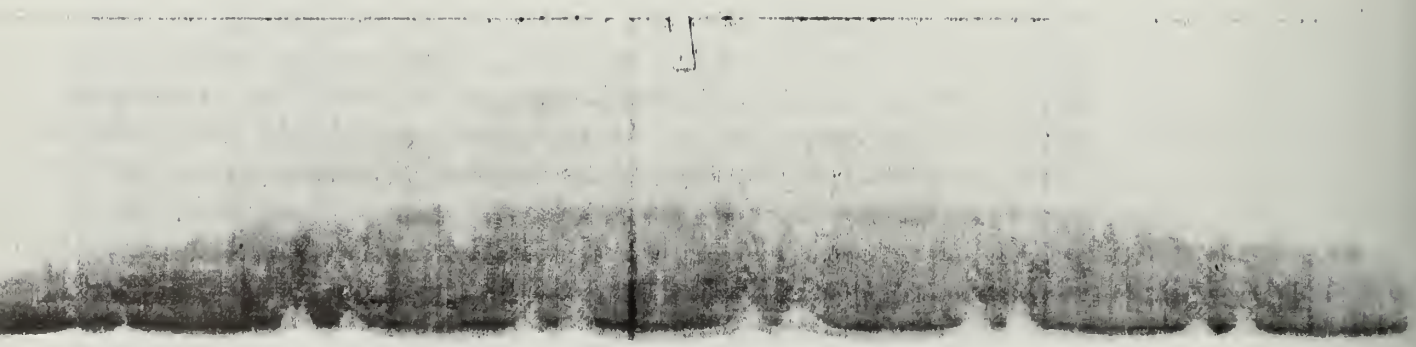

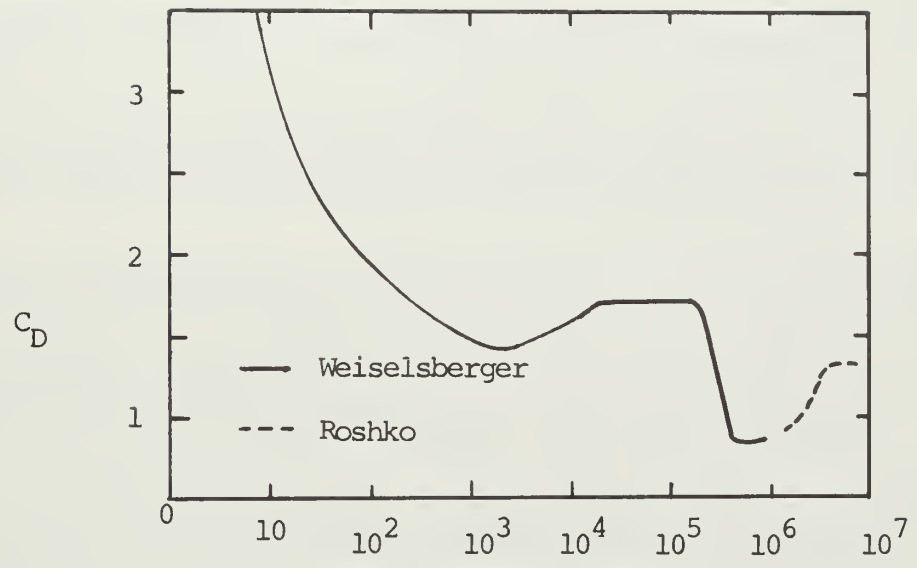

Figure 5.2 Measured Circular Cylinder Drag Coefficients.

BIBLIOGRAPHY

1. A. Acrivos, M. J. Shah, and E. E. Petersen, "Momentum and Heat Transfer in Laminar Boundary Layer Flows of Non-Newtonian Fluids Past External Surfaces", A.I.Ch.E. Journal 6, 312 (1960).

2. D. L. Bacon and E. G. Reid. "The Resistance of Spheres in Wind Tunnels and in Air," N.A.C.A. Report No. 185 (1924).

3. R. B. Bird, W. E. Stewart, and E. N. Lightfoot. Transport Phenomena (John Wiley and Sons, New York, 1960).

4. G. D. Bizzell and J. C. Slattery, "Non-Newtonian Boundary Layer Flow," Chemical Engineering Science 17, 777 (1962).

5. J. H. Chenard, "Drag of Spheres in Dilute Aqueous Solutions of Poly(ethylene oxide) Within the Region of the Critical Reynolds Number," Thesis, Naval Postgraduate School, Monterey, California (1967).

6. J. C. De Vos, "A New Determination of the Emissivity of Tungsten Ribbon". Physica, 10, 669 (1954).

7. C. D. Dever, R. J. Harbour, and W. F. Seifert, "Method of Decreasing Friction Loss in Flowing Fluids," U. S. Patent No. 3,023,760, Filed 1961 (1962).

8. D. W. Dodge and A. B. Metzner, "Turbulent Flow of Non-Newtonian Systems," A.I.Ch.E. Journal 5, 189 (1959).

9. A. G. Fabula, "The Toms Phenomenon in the Turbulent Flow of Very Dilute Polymer Solutions," Proceedings of the Fourth International Congress on Rheology, (Interscience Publishers, New York, 1965).

10. R. E. Forester and P. S. Francis, "Development of a Fluid Concentrated Dispersion of a Water Soluble Polymer Capable of Reducing the Friction of Water under Turbulent Conditions," North Star Research and Development Institute, Tech. Report to David Taylor Model Basin (1966).

11. H. Fröhlich and R. Sack, "Theory of the Rheological Properties of Dispersions," Proceedings of the Royal Society A 185, 415 (1946).

12. G. E. Gadd, "Reduction of Turbulent Friction in Liquids by Dissolved Additives," Nature 212, 874 (1966).

13. G. E. Gadd, "Turbulence Damping and Drag Reduction Produced by Certain Additives in Water," Nature 206, 463 (1965).

14. R. J. Goldstein and D. K. Kreid, "Measurement of Laminar Flow Development in a Square Duct Using a Laser-Doppler Flow Meter," Journal of Applied Mechanics 34, 813 (1967).

15. S. Goldstein, Modern Developments in Fluid Dynamics,Vol II, (Dover Publications, Inc., New York, 1965).

16. Y. Goren and J. F. Norbury. "Turbulent Flow of Dilute Aqueous Polymer Solutions," Journal of Basic Engineering 89, 814 (1967).

17. P. S. Granville, "The Frictional Resistance and Boundary Layer of Flat Plates in Non-Newtonian Fluids," Journal of Ship Research 6, 43, (1962).

18. L. Greiner, Underwater Missile Propulsion, (Compass Publications, Inc., Arlington, Va., 1967).

19. J. Happel and B. J. Byrne, "Motion of a Sphere and Fluid in a Cylindrical Tube," Industrial and Engineering Chemistry 46, 1181 (1954).

20. M. F. Hayes, "Drag Coefficients of Spheres Falling in Dilute Aqueous Solutions of Long-Chain Macromolecules," Thesis, Naval Postgraduate School, Monterey, California (1966).

21. H. C. Hershey and J. L. Zakin, "Existence of Two Types of Drag Reduction in Pipe Flow of Dilute Polymer Solutions," Industrial and Engineering Chemistry Fundamentals 6, 381 (1967).

22. S.F. Hoerner, Fluid Dynamic Drag. (Dr ing S. F. Hoerner, Midland Park, New Jersey, 1965).

23. J. W. Hoyt and A. G. Fabula, "The Effect of Additives of Fluid Friction," Fifth Symposium on Naval Hydrodynamics. Bergin, Norway, 1965.

24. V. G. Jensen, "Viscous Flow Round a Sphere at Low Reynolds Numbers (< 40) Proceedings of the Royal Society of London 249A, (1959).

25. T. Kowalski, "Reduction of Frictional Drag by Non-Newtonian Additives," Naval Engineers Journal, 78, 293 (1966).

26. T. G. Lang and H. V. L. Patrick," Drag of Blunt Bodies in Polymer Solutions," Naval Ordnance Test Station TP4379.

27. T. McClanahan and P. J. Ridgely, "Drag of Circular Cylinders in Dilute Aqueous Solutions of Poly(ethylene oxide) for Flows Characterized by Laminar Boundary Layer Separation," Thesis, Naval Postgraduate School, Monterey, California (1968).

28. J. S. McNown, H. M. Lee, M. B. McPherson, and S. M. Engez, "Influence of Boundary Proximity on the Drag of Spheres," Proceedings of the Seventh International Congress of Applied Mechanics, 1948.

29. C. W. McGary, Jr., "Degradation of Poly(ethylene oxide)," Journal of Polymer Science, 46, 51 (1960).

30. E. W. Merrill, H. S. Mickley, A. Ram, "Degradation of Polymers in Solution Induced by Turbulence and Droplet Formation," Journal of Polymer Science 62, S-109 (1962).

31. E. W. Merrill, K. A. Smith, and R. Y. C. Chung, "Drag Augmentation by Polymer Addition," A.I.Ch.E. Journal 12, 809 (1966).

32. A. B. Metzner and M. G. Park, "Turbulent Flow Characteristics of Viscoelastic Fluids," Journal of Fluid Mechanics, 20, 291 (1964).

33. F. Odar, "Verification of the Proposed Equation for Calculation of the Forces on a Sphere Accelerating in a Viscous Fluid," Journal of Fluid Mechanics 25, 591 (1966).

34. F. Odar and W. S. Hamilton, "Forces on a Sphere Accelerating in a Viscous Fluid," Journal of Fluid Mechanics, 18, 302 (1964).

35. J. G. Oldroyd, D. J. Strawbridge, and B. A. Toms, "A Coaxial Cylinder Elastoviscometer," Proceedings of the Physical Society, B64, 44 (1951).

36. G. M. Powell, III and F. E. Bailey, "Poly(ethylene oxide)", Encyclopedia of Chemical Technology, Second Supplement, Kirk-Othmer, (Interscience Encyclopedia, Inc., New York, 1960).

37. G. T. Pruit and H. R. Crawford, "Effect of Molecular Weight and Segmental Constitution on the Drag Reduction of Water Soluble Polymers," Final Report, Cont. No. Nonr-4306(00) (1965).

38. G. T. Pruit, B. Rosen, and H. R. Crawford, "Effect of Polymer Coiling on Drag Reduction," Technical Report, Cont. No. Nonr 4306 (00) (1966).

39. A. Ram, E. Finkelstein, and C. Elata, "Reduction of Friction in Oil Pipelines by Polymer Additives," Industrial and Engineering Chemistry, Process Design and Development 6, 309 (1967).

40. A. Roshko, "Experiments on the Flow Past a Circular Cylinder at Very High Reynolds Number," Journal of Fluid Mechanics 10, 345 (1961).

41. M. A. Ruszczycky, "Sphere Drop Tests in High Polymer Solutions," Nature, 206, 614 (1965).

42. J. V. Sanders, "Drag Coefficients of Spheres in Poly(ethylene oxide) Solutions," International Shipbuilding Progress 14, 140 (1967).

43. H. Schlichting, Boundary Layer Theory, 4th Ed., (McGraw-Hill Book Company, Inc., New York, 1960).

44. E. T. Severs, Rheology of Polymers, (Reinhold Publishing Corp., New York, 1962).

45. R. G. Shaver and E. W. Merrill, "Turbulent Flow of Pseudoplastic Polymer Solutions in Straight Cylindrical Tubes," A.I.Ch.E. Journal 5, 181 (1959).

46. H. Shin, "Reduction of Drag and Turbulence by Dilute Polymer Solutions", Sc. D. Thesis, MIT (1965).

47. W. P. Siegmund, "Fiber Optics". Applied Optics and Optical Engineering, Edited by R. Kingslake, (Academic Press, New York, 1967).

48. A. H. P. Skelland, Non-Newtonian Flow and Heat Transfer, (John Wiley and Sons, Inc., New York, 1967).

49. J. C. Slattery and R. B. Bird, "Non-Newtonian Flow Past a Sphere," Chemical Engineering Science 16, 231 (1961).

50. S. Thurston and R. D. Jones," Experimental Model Studies of Non-Newtonian Soluble Coatings for Drag Reduction," Journal of Aircraft 2, 122 (1965).

51. B. A. Toms, "Some Observations on the Flow of Linear Polymer Solutions Through Straight Tubes at Large Reynolds Numbers," Proceedings of the First International Congress on Rheology, North Holland Publishing Company, Amsterdam, 1949.

52. B. A. Toms and D. J. Strawbridge, "Elastic and Viscous Properties of Dilute Solutions of Polymethylmethacrylate in Organic Liquids," Transactions of the Faraday Society 10, 1225 (1953).

53. L. B. Torobin and W. H. Gauvin, "Fundamental Aspects of Solids-Gas Flow: Part I, Introductory Concepts and Idealized Sphere Motion in Viscous Regime," Canadian Journal of Chemical Engineering 37, 129 (1959).

54. L. B. Torobin and W. H. Gauvin, "Fundamental Aspects of Solids-Gas Flow: Part II. The Sphere Wake in Steady Laminar Fluids," Canadian Journal of Chemical Engineering 37, 167 (1959).

55. L. B. Torobin and W. H. Gauvin, "Fundamental Aspects of Solids-Gas Flow: Part IV. The Effects of Particle Rotation, Roughness, and Shape," Canadian Journal of Chemical Engineering 38, 142 (1960).

56. L. B. Torobin and W. H. Gauvin, "Fundamental Aspects of Solids-Gas Flow: Part V. The Effects of Fluid Turbulence on the Particle Drag Coefficient," Canadian Journal of Chemical Engineering 38, 189 (1960).

57. R. M. Turian, "An Experimental Investigation of the Flow of Aqueous Non-Newtonian High Polymer Solutions Past a Sphere". A.I.Ch.E. Journal, 13, 999, (1967).

58. Union Carbide Corp., Chemicals Div. "Friction-Reducing Agent Improves Water Flow." Chem. Eng. 73, 36, (1966).

59. Union Carbide Chemicals Company, "How to Dissolve Polyox Water Soluble Resins," Advance Technical Information Booklet F-41101A, December, 1964.

60. L. Van Wijngaarden, "Asymptotic Solution of the Laminar Boundary Layer Equations for a Non-Newtonian Fluid," Journal of Ship Research 9, 37 (1965).

61. V. A. Vanoni, "Transportation of Suspended Sediment by Water," Transactions of American Society of Civil Engineers III (1946).

62. W. M. Vogel and A. M. Patterson, "An Experimental Investigation of the Effect of Additives Injected into the Boundary Layer of an Underwater Body," Fifth Symposium on Naval Hydrodynamics, Bergen, Norway, September 1964.

63. M. Walsh, "Theory of Drag Reduction in Dilute High-Polymer Flows," International Shipbuilding Progress 14, 134 (1967).

64. A. White, "Effect of Polymer Additives on Boundary Layer Separation and Drag of Submerged Bodies," Nature 211, 1390 (1966).

65. D. A. White, "Drag Coefficients for Spheres in High Reynolds Number Flow of Dilute Solutions of High Polymers," Nature 212, 277 (1966).

66. F. M. White, "An Analysis of the Effect of a Polymer Additive on Turbulent Wall Friction and Pressure Fluctuations," Navy Underwater Sound Laboratory, USC Report No. 881, 29 December 1967.

67. M. C. Williams, "Correlation of Stress Data in Viscoelastic Polymer Solutions," A.I.Ch.E. Journal 14, 360 (1968).

APPENDIX A

```
C                 PROGRAM FOR COMPUTING INTERVAL VELOCITIES,
C                 AVERAGE VELOCITIES, DRAG COEFFICIENTS,AND
C                 REYNOLDS NUMBERS FOR FALLING SPHERES.
C
      DIMENSION A(100,11),V(11),AREF(100,11),S(11),SUMCD(10),SUMRN(10),
     C            CDSQ(10),RNSQ(10),R(10),CDAVG(10),RNAVG(10),CDDV(10),
     C            RNDV(10)
      READ(5,60)L,IRUN,RHOW,VISC
C                 L IS NUMBER OF RUNS
C                 IRUN IS FIRST SEQUENTIAL RUN NUMBER RECORDED ON REEL
C                 OF MAG TAPE FOR RUNS INCLUDED IN THIS COMPUTATION.
C                 RHOW IS DENSITY OF WATER IN KG/M**3
C                 VISC IS VISCOSITY OF WATER
      WRITE(6,60)L,IRUN,RHOW,VISC
      READ(5,10)((A(K,I),I=1,11),K=1,L),((AREF(K,I),I=1,11),K=1,L)
C                 A(K,I) IS TIME, EXPRESSED IN MILLIMETERS, BETWEEN PULSES
C                 OF INTERVAL I OF RUN K READ FROM OSCILLOGRAM TAKEN AT
C                 125 MM/SEC OR 0.008 SEC/MM.
C                 AREF(K,I) IS PERIOD IN MM OF REFERENCE SIGNAL
C                 IN INTERVAL I OF RUN K READ FROM OSCILLOGRAM TAKEN AT
C                 125 MM/SEC OR 0.008 SEC/MM.
      WRITE(6,10)((A(K,I),I=1,11),K=1,L),((AREF(K,I),I=1,11),K=1,L)
      DO 4 I=1,10
      SUMCD(I)=0
      SUMRN(I)=0
      CDSQ(I)=0
      RNSQ(I)=0
      CDAVG(I)=0
      RNAVG(I)=0
      CDDV(I)=0
      RNDV(I)=0
    4 R(I)=0
      S(1)=.108
      S(2)=.108
      S(3)=.109
      S(4)=.110
      S(5)=.110
      S(6)=.108
      S(7)=.110
      S(8)=.107
      S(9)=.111
      S(10)=.110
      S(11)=.109
      G=9.807
      DO 93 K=1,L
      KRUN=IRUN+K-1
      IF(KRUN.GE.208) KRUN=KRUN+5
      XISQ=0
```

```
      SUM=0
      DO 3 I=1,11
      IF(AREF(K,I))3,3,2
    2 AREF(K,I)=(AREF(K,I)*.008)/10.
      SUM=SUM+AREF(K,I)
      XISQ=XISQ+AREF(K,I)**2
    3 CONTINUE
      TREF=SUM/11.
C               TREF IS MEAN REFERENCE TIME OBSERVED DURING PLAYBACK
C               OF MAGNETIC TAPE DATA CORRECTED FOR PLAYBACK AT 1/10
C               SPEED.
      TREFSQ=(XISQ-11.*TREF**2)/10.
      TREFAB=ABS(TREFSQ)
      TREFDV=SQRT(TREFAB)
      NUM=TREF*1.E3+.5
      TNUM=NUM*1.E-03
C               TNUM IS CALCULATED VALUE OF REFERENCE TIME, OF PERIOD
C               OF REFERENCE SIGNAL, RECORDED ON MAG TAPE.  A DIFFERENT
C               REFERENCE TIME IS USED FOR EACH SPHERE.
C
C     SPHERE NUMBER=NUM    REF TIME,SECONDS      REF SIGNAL FREQ,HZ
C                          (ACTUALLY RECORDED)
C                    1          0.001                 1000.0
C                    2          0.002                  500.0
C                    3          0.003                  333.3
C                    4          0.004                  250.0
C                    5          0.005                  200.0
C                    6          0.006                  166.7
C                    7          0.007                  142.9
C                    8          0.008                  125.0
C                    9          0.009                  111.1
C                   10          0.010                  100.0
C
C               COMPUTE INTERVAL VELOCITIES,V(I), MEAN VELOCITIES,VAVG,
C               AND STANDARD DEVIATION OF MEAN VELOCITIES,VDV.
C               VELOCITIES ARE IN METERS/SECOND.  TIME IS IN SECONDS.
      RI=1.
      VAVG=0
      VISQ=0
      DO 17 I=1,11
      IF(A(K,I))17,17,12
   12 A(K,I)=(A(K,I)*.008*TNUM)/(TREF*10.)
      V(I)=S(I)/A(K,I)
      VREL=(VAVG-V(I))/V(I)
      TEST=ABS(VREL)
      IF(TEST-.05)13,13,6
    6 IF(I-1)7,7,8
    7 VAVG=V(I)
```

```
      WRITE(6,70) TEST,I
      GO TO 16
    8 M=I-1
      VAVG=(V(M)+V(I))/2.
      WRITE(6,70) TEST,I
      GO TO 16
   13 RI=RI+1.
      VAVG=(VAVG*(RI-1.)+V(I))/RI
   16 VISQ=VISQ+V(I)**2
   17 CONTINUE
      VDVSQ=(VISQ-11.*VAVG**2)/10.
      VDVAB=ABS(VDVSQ)
      VDV=SQRT(VDVAB)
      IF(VAVG)93,93,18
   18 VDEV=.05*VAVG
C
C                COMPUTE DRAG COEFFICIENT, CDRAG, REYNOLDS NUMBER, REYNUM,
C                AND LOGARITHMS OF CDRAG AND REYNUM
   21 IF(NUM)93,93,23
   23 GO TO (5,15,25,35,45,55,65,75,85,95),NUM
    5 D=.101322
      RHOS=8416.3
      GO TO 88
   15 D=.088863
      RHOS=7950.
      GO TO 88
   25 D=.075981
      RHOS=7952.4
      GO TO 88
   35 D=.063497
      RHOS=8437.0
      GO TO 88
   45 D=.100993
      RHOS=2782.8
      GO TO 88
   55 D=.088759
      RHOS=2775.8
      GO TO 88
   65 D=.050584
      RHOS=8460.9
      GO TO 88
   75 D=.076214
      RHOS=2780.5
      GO TO 88
   85 D=.063468
      RHOS=2697.5
      GO TO 88
   95 D=.050827
```

```
      RHOS=2779.6
   88 DENSW=(RHOS/RHOW)-1.
      CDRAG=(4.*D*DENSW*G)/(3.*VAVG**2)
      VISCKN=(VISC*.1)/RHOW
C                VISC IS ABSOLUTE VISCOSITY IN POISE
C                VISCKN IS KINEMATIC VISCOSITY IN M**2/SEC
      REYNUM=(D*VAVG)/VISCKN
      CDLOG=ALOG10(CDRAG)
      RNMLOG=ALOG10(REYNUM)
      IF(VDV-VDEV)96,96,91
   91 WRITE(6,40)KRUN,NUM
      DO 92 I=1,11
      CDRAGI=(4.*D*DENSW*G)/(3.*V(I)**2)
      RYNUMI=(D*V(I))/VISCKN
   92 WRITE(6,20)I,V(I),CDRAGI,RYNUMI
C                CDRAGI IS A VALID INTERVAL DRAG COEFFICIENT ONLY IF
C                THE VELOCITY IS STEADY AND SPHERE IS NOT ACCELERATED.
C                RYNUMI IS CORRESPONDING INTERVAL REYNOLDS NUMBER.
   96 WRITE(6,50)
      WRITE(6,30)KRUN,TNUM,TREF,TREFDV,VAVG,VDV,CDRAG,REYNUM,CDLOG,
     C          RNMLOG
C                THESE LOGICAL IF STATEMENTS CAUSE THOSE RUNS WHICH
C                SHOULD NOT BE AVERAGED IN CDRAG OR RNAVG TO BE EXCLUDED
C                IN THE AVERAGES.
      IF((KRUN.GE.201).AND.(KRUN.LE.203)) GO TO 87
      IF((KRUN.GE.213).AND.(KRUN.LE.215)) GO TO 87
      IF((KRUN.GE.219).AND.(KRUN.LE.221)) GO TO 87
      IF(KRUN.EQ.225) GO TO 87
      GO TO 89
   87 WRITE(6,100)
      GO TO 93
   89 SUMCD(NUM)=SUMCD(NUM)+CDRAG
      SUMRN(NUM)=SUMRN(NUM)+REYNUM
      R(NUM)=R(NUM)+1.
      CDSQ(NUM)=CDSQ(NUM)+CDRAG**2
      RNSQ(NUM)=RNSQ(NUM)+REYNUM**2
   93 CONTINUE
      WRITE(6,80)
      DO 99 I=1,10
      IF(R(I))99,99,94
   94 CDAVG(I)=SUMCD(I)/R(I)
      RNAVG(I)=SUMRN(I)/R(I)
      IF(R(I)-1.)99,99,97
   97 CDDV(I)=SQRT((CDSQ(I)-R(I)*CDAVG(I)**2)/(R(I)-1.))
      RNDV(I)=SQRT((RNSQ(I)-R(I)*RNAVG(I)**2)/(R(I)-1.))
      WRITE(6,90) I,CDAVG(I),CDDV(I),RNAVG(I),RNDV(I),R(I)
   99 CONTINUE
  100 FORMAT(11F7.3)
```

```
 20 FORMAT(52X,1I3,12X,1F6.3,8X,1F6.3,8X,1E10.3)
 30 FORMAT(/,4X,1I4,4X,1E11.4,4X,1E11.4,4X,1E11.4,4X,1F6.3,4X,
   C         1E10.3,4X,1F6.3,4X,1E10.3,4X,1F7.4,4X,1F7.4,/)
 40 FORMAT(//,15X,5HRUN= ,1I4,5X,12HSPHERE NUM= ,1I3,5X,8HINTERVAL,
   C         10X,4HV(I),10X,6HCDRAG(I,10X,6HREYNUM(I,/)
 50 FORMAT(/,6X,1HK,7X,4HTNUM,11X,4HTREF,11X,6HTREFDV,8X,4HVAVG,8X,
   C         3HVDV,9X,5HCDRAG,6X,6HREYNUM,7X,5HCDLOG,4X,6HRNMLOG,/)
 60 FORMAT(2I5,2E11.4)
 70 FORMAT(/,16X,6HTEST= ,1E10.3,16X,3HI= ,1I3)
 80 FORMAT(//,8X,13HSPHERE NUMBER,6X,8HCDAVG(I),13X,7HCDDV(I),16X,
   C         8HRNAVG(I),16X,7HRNDV(I),15X,4HR(I),/)
 90 FORMAT(/,13X,1I2,13X,1F6.3,13X,1E10.3,13X,1E10.3,13X,1E10.3,
   C         13X,1F5.1)
100 FORMAT(30X,43H(THIS RUN NOT INCLUDED IN CDAVG AND RNAVG.),//)
    STOP
    END
```

INITIAL DISTRIBUTION LIST

		No. Copies
1.	Defense Documentation Center Cameron Station Alexandria, Virginia 22314	20
2.	Library Naval Postgraduate School Monterey, California 93940	2
3.	Naval Ship Systems Command Navy Department Washington, D. C. 20360	1
4.	Professor James V. Sanders Department of Physics Naval Postgraduate School Monterey, California 93940	10
5.	CDR Edgar F. Woolery 4500 S. Jackson Drive Springfield, Missouri 65804	2
6.	Mr. William Smith Department of Physics Naval Postgraduate School Monterey, California 93940	1
7.	Dr. J. W. Hoyt Head of Propulsion Division Naval Undersea Warfare Center 3202 E. Foothill Blvd. Pasadena, California 91107	1
8.	Dr. A. G. Fabula Naval Undersea Warfare Center 3202 E. Foothill Blvd. Pasadena, California 91107	1
9.	Professor H. A. Dahl Department of Physics Naval Postgraduate School Monterey, California 93940	1
10.	Vice Admiral Roger Brard Bassin D'Essais Des Carenes 6 Boulevard Victor (XV) Paris, France	1

DOCUMENT CONTROL DATA - R & D

(Security classification of title, body of abstract and indexing annotation must be entered when the overall report is classified)

1. ORIGINATING ACTIVITY *(Corporate author)*
Naval Postgraduate School
Monterey, California 93940

2a. REPORT SECURITY CLASSIFICATION
Unclassified

2b. GROUP

3. REPORT TITLE
Drag of Free-Falling Spheres in Dilute Aqueous Solutions of Poly(ethylene oxide) for Reynolds Numbers Above the Critical Value

4. DESCRIPTIVE NOTES *(Type of report and inclusive dates)*
Thesis, December 1968

5. AUTHOR(S) *(First name, middle initial, last name)*
Edgar F. Woolery

6. REPORT DATE
December 1968

7a. TOTAL NO. OF PAGES
93

7b. NO. OF REFS
67

8a. CONTRACT OR GRANT NO.
N/A

b. PROJECT NO.
N/A

c.
N/A

d.

9a. ORIGINATOR'S REPORT NUMBER(S)
N/A

9b. OTHER REPORT NO(S) *(Any other numbers that may be assigned this report)*
N/A

10. DISTRIBUTION STATEMENT
This document has been approved for public release and sale; its distribution is unlimited.

11. SUPPLEMENTARY NOTES
N/A

12. SPONSORING MILITARY ACTIVITY
Naval Postgraduate School
Monterey, California

13. ABSTRACT

Drag of free-falling spheres in water and in dilute aqueous solutions of poly(ethylene oxide) was measured by ejecting the spheres near terminal velocity in a fluid-filled tank. Polymer additive concentrations tested were 1000 wppm, 200 wppm, and 100 wppm. The results agree with previous investigations, available only for subcritical Reynolds numbers, in that the drag coefficient decreases with increasing water Reynolds number and decreasing polymer concentration. It is shown that in the polymer solutions abrupt decrease in drag coefficient occurs at about the same Reynolds number (3×10^5) as the critical value in water. For Reynolds numbers greater than the critical value, the drag was still less than in water and increased slightly with increasing polymer concentration. At Reynolds numbers between 7 and 8×10^5, the drag coefficients for all polymer concentrations, including water, abruptly increased to nearly a common value at the upper limit of this investigation.

14 KEY WORDS	LINK A		LINK B		LINK C	
	ROLE	WT	ROLE	WT	ROLE	WT
Drag reduction						
Spheres						
Polyethylene oxide						
Optical velocimeter						
Critical Reynolds number						